

**THE DESIGN OF FINITE IMPULSE RESPONSE (FIR)
WAVEFIELD EXTRAPOLATION FILTERS**

BY
MUHAMMAD MUZAMMAL NASEER

A Thesis Presented to the
DEANSHIP OF GRADUATE STUDIES
KING FAHD UNIVERSITY OF PETROLEUM & MINERALS
DHAHRAN, SAUDI ARABIA

In Partial Fulfillment of the
Requirements for the Degree of

MASTER OF SCIENCE

In

ELECTRICAL ENGINEERING

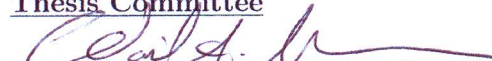
DECEMBER, 2013

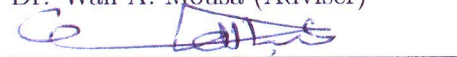
KING FAHD UNIVERSITY OF PETROLEUM & MINERALS
DHAHRAN 31261, SAUDI ARABIA

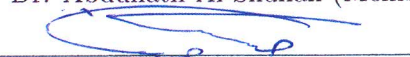
DEANSHIP OF GRADUATE STUDIES

This thesis, written by **MUHAMMAD MUZAMMAL NASEER** under the direction of his thesis adviser and approved by his thesis committee, has been presented to and accepted by the Dean of Graduate Studies, in partial fulfillment of the requirements for the degree of **MASTER OF SCIENCE IN ELECTRICAL ENGINEERING**.

Thesis Committee


Dr. Wail A. Mousa (Adviser)


Dr. Abdullatif Al-Shuhail (Member)


Dr. Tareq Al-Naffouri (Member)



Dr. Ali Ahmad Al-Shaikhi
Department Chairman

Dr. Salam A. Zummo
Dean of Graduate Studies

14/1/14
Date



To my beloved parents, sister and brothers..

ACKNOWLEDGMENTS

With the name of Allah, the most Beneficent, the most Merciful Blessings and grace on Prophet Muhammad, Ahl-e-bayt, Companions of Prophet and anyone who follows him.

First of all, I want to thank my family, especially my mother and father, for their unconditional love, support and prayers. I can never forget their efforts and sacrifices that made me able to earn this post-graduate degree.

I am grateful to KFUPM university for giving me the scholarship and providing me the opportunity to learn in a dynamic environment. I would also like to thank Dr. Wail A. Mousa for allowing me to pursue my masters thesis with him and providing complete support and guidance to accomplish my thesis requirements. It was a nice experience to work under his supervision because he was completely involved in my work. In addition to his technical support, I would like to specifically thank him for his effort to improve my writing and presentation skills. In addition to my supervisor, I would also like to thank my thesis committee members, Dr. Abdullatif A.Al-Shuhail and Dr. Tareq Y.Al-Naffouri for rigorously reviewing and improving my thesis work.

TABLE OF CONTENTS

ACKNOWLEDGEMENTS	ii
LIST OF TABLES	vi
LIST OF FIGURES	vii
ABSTRACT (ENGLISH)	xii
ABSTRACT (ARABIC)	xiv
CHAPTER 1 INTRODUCTION	1
1.1 Introduction	1
1.2 Thesis Contributions	2
1.3 Thesis Organization	3
CHAPTER 2 SEISMIC IMAGING AS A FILTERING PROCESS	4
2.1 Introduction	4
2.2 One-dimensional extrapolation filters	5
2.3 Subsurface Image	10
2.4 Summary	14
CHAPTER 3 DESIGN OF ONE-DIMENSIONAL FIR WAVE- FIELD EXTRAPOLATION FILTER VIA LINEAR COMPLI- MENTARITY PROBLEM APPROACH	15
3.1 Introduction	16

3.2	The design of LCP based FIR extrapolation filters	18
3.2.1	Design Algorithm	24
3.3	Simulation Results	26
3.4	Application to SEG/EAGE Salt Model	28
3.5	Summary	42
CHAPTER 4 ONE DIMENSIONAL WAVEFIELD EXTRAPO-		
LATION FILTER VIA L_1 ERROR APPROXIMATION		43
4.1	Introduction	43
4.2	Problem Formulation	44
4.2.1	Design Algorithm	46
4.3	Simulation Results	46
4.4	Application to SEG/EAGE Salt Model	49
4.5	Summary	61
CHAPTER 5 CONCLUSION AND FUTURE WORK		62
5.1	Future Work	63
5.1.1	Efficient LCP Solvers	64
5.1.2	Optimal tradeoff between different norms	64
APPENDIX A LINEAR COMPLIMENTARITY PROBLEM		66
A.1	Mathematical Structure of LCP	66
A.2	Source Problems	67
A.2.1	Application to Quadratic Programming	67
A.3	Algorithms	70
A.3.1	Homotopy Approach	70
A.3.2	Lemke the path following Algorithm	72
APPENDIX B CONVEXITY AND K-T CONDITIONS		79
B.1	Convex Set	79
B.1.1	Theorem: 1	80
B.1.2	Theorem: 2	80

B.2 The KUHN-TUCKER Conditions	80
REFERENCES	82
VITAE	89

LIST OF TABLES

3.1	Comparison of CPU (core-i5) design time for designing 1-D FIR extrapolation filter with 25 and 35 coefficients designed via LCP-Lemke and LCP-Fisher-Newton algorithms	28
-----	--	----

LIST OF FIGURES

2.1	(a) Magnitude response of the desired 2-D extrapolation filter, and (b) phase response of the desired 2-D extrapolation filter	8
2.2	(a) Magnitude and (b) phase response of the ideal 1-D extrapolation filter	9
2.3	Example of a 1-D FIR $w-x$ extrapolation filter requirements. (a) A noncausal spatial impulse response (operator) with even symmetry and (b) a short-length FIR $w-x$ extrapolation filter coefficients for accuracy. Due to the heterogeneity within a layer, the velocity can also vary horizontally. At every lateral position, a new filter is used to perform extrapolation on the data from one depth level to another one. Within the filter length, the medium is assumed to be homogeneous. (c) Accurate magnitude wavenumber response and (d) an accurate passband phase response [1].	11
3.1	LCP based work flow of the algorithm to design $f-x$ FIR wavefield extrapolation filters.	25
3.2	(a) Magnitude and (b) phase response of 1-D extrapolation filter designed by LCP-Lemke, LCP-Fisher, the modified Taylor series [2] and MPOCS [3] (c) and (d) show the passband magnitude and phase errors, respectively.	26

3.3	(a) Magnitude and (b) phase response of 1-D extrapolation filter designed by LCP-Lemke and LCP-Fisher, the modified Taylor series [2] and MPOCS [3] (c) and (d) show the passband magnitude and phase errors, respectively.	27
3.4	Shows the SEG/EAGE salt velocity model. Velocity changes from minimum value 1,500 m/s that correspond to the acoustics speed in water represented by black color to maximum value 4,500 m/s that correspond to the acoustics speed in salt represented by white color.	29
3.5	Shows the zero-offset section of the SEG/EAGE Salt Model, generated based on finite difference method [4]. Performance of LCP has been tested on this data set.	30
3.6	Set of designed $f - x$ FIR extrapolation filters in the frequency wavenumber domain with $N = 25$ (a) and (b) show the magnitude and phase responses of Lemke's algorithm, (c) and (d) show the magnitude and phase responses of Fisher's algorithm, (e) and (f) show error between the frequency wavenumber responses for the magnitude and phase responses, respectively.	31
3.7	Set of designed $f - x$ FIR extrapolation filters in the frequency wavenumber domain with $N = 35$ (a) and (b) show the magnitude and phase responses of Lemke's algorithm, (c) and (d) show the magnitude and phase responses of Fisher's algorithm, (e) and (f) show error between the frequency wavenumber responses for the magnitude and phase responses, respectively.	32
3.8	Extrapolated SEG/EAGE salt model using Lemke algorithm with 25-coefficients.	33
3.9	Extrapolated SEG/EAGE salt model using Fisher-Newton algorithm with 25-coefficients.	34
3.10	Extrapolated SEG/EAGE salt model using Modified Taylor Series [2] with 25-coefficients.	35

3.11	Extrapolated SEG/EAGE salt model using Modified Projection Onto Convex Sets (MPOCS) [3] with 25-coefficients.	36
3.12	Extrapolated SEG/EAGE salt model using Lemke algorithm with 35-coefficients.	37
3.13	Extrapolated SEG/EAGE salt model using Fisher-Newton algo- rithm with 35-coefficients.	38
3.14	Details of an area with different dips (lateral position of 7500 – 9750m and depth of 1200 – 1800m) using (a) MPOCS [3] ($N = 25$) (b) Modified Taylor Series [2] ($N = 25$) (c) LCP-Lemke ($N = 25$), (d) LCP-Fisher ($N = 25$), (e) LCP-Lemke ($N = 35$), (f) LCP- Fisher ($N = 35$)	39
3.15	Details of an area with steep dips on the left flank of the salt model (lateral position of 6000 – 8000m and depth of 1800 – 2800m) using (a) MPOCS [3] ($N = 25$) (b) Modified Taylor Series [2] ($N = 25$)(c) LCP-Lemke ($N = 25$), (d) LCP-Fisher ($N = 25$), (e) LCP-Lemke ($N = 35$), (f) LCP-Fisher ($N = 35$)	40
3.16	Details of a structurally challenging sub-salt area (lateral position of 6500 – 8500m and depth of 3400 – 4000m) using (a) MPOCS [3] ($N = 25$) (b) Modified Taylor Series [2] ($N = 25$)(c) LCP-Lemke ($N = 25$), (d) LCP-Fisher ($N = 25$), (e) LCP-Lemke ($N = 35$), (f) LCP-Fisher ($N = 35$)	41
4.1	L_1 error approximation based work flow of the algorithm to design $f - x$ FIR wavefield extrapolation filters.	46
4.2	(a) Magnitude and (b) phase response of 1-D extrapolation filter de- signed by L_1 error approximation with and without weights, LCP- Lemke and L_1 norm [5] approach, (c) and (d) show the passband magnitude and phase errors, respectively.	47

4.3	(a) Magnitude and (b) phase response of 1-D extrapolation filter designed by L_1 error approximation with and without weights, LCP-Lemke and L_1 norm [5] approach, (c) and (d) show the passband magnitude and phase errors, respectively.	48
4.4	Set of designed $f - x$ FIR extrapolation filters in the frequency-wavenumber domain with $N = 25$ (a) and (b) show the magnitude and phase responses of L_1 error approximation (c) and (d) show the magnitude and phase responses of weighted L_1 error approximation and (e) and (f) show the magnitude and phase responses of L_1 norm [5], respectively.	50
4.5	Set of designed $f - x$ FIR extrapolation filters in the frequency-wavenumber domain with $N = 35$ (a) and (b) show the magnitude and phase responses of L_1 error approximation (c) and (d) show the magnitude and phase responses of weighted L_1 error approximation and (e) and (f) show the magnitude and phase responses of L_1 norm [5], respectively.	51
4.6	Extrapolated SEG/EAGE salt model using L_1 error approximation with 25-coefficients.	52
4.7	Extrapolated SEG/EAGE salt model using weighted L_1 error approximation with 25-coefficients.	53
4.8	Extrapolated SEG/EAGE salt model using L_1 norm [5] with 25-coefficients.	54
4.9	Extrapolated SEG/EAGE salt model using L_1 error approximation with 35-coefficients.	55
4.10	Extrapolated SEG/EAGE salt model using weighted L_1 error approximation with 35-coefficients.	56
4.11	Extrapolated SEG/EAGE salt model using L_1 norm [5] with 35-coefficients.	57

4.12	Details of an area with different dips (lateral position of 7500 – 9750m and depth of 1200 – 1800m) using (a) L_1 error norm ($N = 25$), (b) L_1 error norm ($N = 35$), (c) weighted L_1 error norm ($N = 25$), (d) weighted L_1 error norm ($N = 35$) and (e) L_1 norm [5] ($N = 25$), (f) L_1 norm [5] ($N = 35$)	58
4.13	Details of an area with steep dips on the left flank of the salt model (lateral position of 6000 – 8000m and depth of 1800 – 2800m) using (a) L_1 error norm ($N = 25$), (b) L_1 error norm ($N = 35$), (c) weighted L_1 error norm ($N = 25$), (d) weighted L_1 error norm ($N = 35$) and (e) L_1 norm [5] ($N = 25$), (f) L_1 norm [5] ($N = 35$)	59
4.14	Details of a structurally challenging sub-salt area (lateral position of 6500 – 8500m and depth of 3400 – 4000m) using (a) L_1 error norm ($N = 25$), (b) L_1 error norm ($N = 35$), (c) weighted L_1 error norm ($N = 25$), (d) weighted L_1 error norm ($N = 35$) and (d) L_1 norm [5] ($N = 25$), (e) L_1 norm [5] ($N = 35$).	60

THESIS ABSTRACT

NAME: Muhammad Muzammal Naseer

TITLE OF STUDY: The design of finite impulse response (FIR) wavefield extrapolation filters

MAJOR FIELD: Electrical Engineering

DATE OF DEGREE: December, 2013

In this research, the problem of complex valued finite impulse response FIR wavefield extrapolation filter design is considered as a linear complementarity problem (LCP). LCP is not an optimization technique as there is no objective function to optimize, however, quadratic programming, one of the applications of LCP, can be used to find an optimal solution for the 1-D FIR wavefield extrapolation filter. Quadratic programs are an extremely important source of applications of LCP, in fact, several algorithms for quadratic programs are based on LCP. This work shows the efforts that are being made to convert the FIR wavefield extrapolation filter design problem into a quadratic program and then finally, to an equivalent linear complementarity problem. There are two families of algorithms available to solve for the LCP: a direct (pivoting based) algorithms, and b indirect (iter-

ative) algorithms . In this study, the LCP has been solved by a direct, Lemke's algorithm, and indirect, Fisher-Newton algorithm. In the explicit depth extrapolation process, FIR wavefield extrapolation filters are used recursively. Hence, the challenge is to design these filters with smallest possible length while keeping passband error as small as possible. To achieve the above design constraints, the problem of designing a 1-D FIR wavefield extrapolation filter has also been studied via L_1 error approximation approach.

Performance of 1-D FIR extrapolation filters designed by the proposed methods has been tested by extrapolating the challenging 2-D SEG/EAGE salt velocity model.

خلاصة أطروحة

مسألة تصميم المرشح الرقمي ذو الاستجابة المحدودة في النظام التخلي للموجات الاستقرائية اعتبرت في هذا البحث باستخدام النظام الخطي التكاملي. بالرغم من أن النظام الخطي التكاملي ليس الأمثل إلا أنه يوحد الخطية التريعية بالإضافة إلى مسألة الإجراءات الجزائية. المسائل التريعية هي مصدر هام لتطبيقات المسألة الخطية التكاملية. في الواقع العديد من الخوارزميات للبرامج التريعية مبني علي المسألة الخطية التكاملية. هذا العمل يبين الجهد المبذول لتحويل تصميم مرشحات الموجات الاستقرائية لبرامج تريعية و ختاماً لمسألة خطية تكاملية مكافئة. هناك عائلتان من الخوارزميات لحل المسألة الخطية التكاملية و هما (أ)خوارزمية مباشرة مبنية على التمحول و (ب) خوارزمية غير مباشرة تكرارية. في حالة مسألة المرشح الاستقرائي الرقمي ذو الاستجابة المحدودة تم حل المسألة الخطية التكاملية باستخدام الخوارزمية المباشرة (خوارزمية ليملك) و الخوارزمية الغير مباشرة (خوارزمية فيشرنيوتن). المرشح الرقمي ذو الاستجابة المحدودة للموجات الاستقرائية استخدم في تقنية مابعد تراكم التصوير بالتكرار لذلك التحدي هو في تصميم هذه المرشحات بأقل طول قدر المستطاع مع ابقاء خطأ المجال المسموح أقل ما يمكن. مسألة تصميم الاستقواء الموجي الزلزالي درس لاستيفاء هذه القيود باستخدام معيار الخطأ (L1) . أداء كلتا الطريقتين المسألة الخطية التكاملية و معيار الخطأ (L1) قورنا بناء على (أ) طول استجابة النبضة و (ب) الخطأ في المجال المسموح و (ج) التوافق في الزوايا المبتوثة العليا. تم توضيح أن المسألة الخطية التكاملية بإمكانها التوفيق في الزوايا المبتوثة العليا على حساب الخطأ في المجال المسموح بينما معيار الخطأ (L1) يمنح خطأ صغير في المجال المسموح لكن يضعف الزوايا المبتوثة العليا. كفاءة التقنيات قد تم توضيحها عن طريق اسقراء نموذج (SEG/EAGE salt velocity) .

CHAPTER 1

INTRODUCTION

1.1 Introduction

Increasing demand for oil and decreasing availability of hydrocarbon deposits are the motivating forces behind the quest to explore and map the earth structure. Oil and natural gas are normally found in what we call reservoir rocks. These reservoirs can be identified by processing seismic reflection data in which seismic imaging is an important step that improves lateral resolution to obtain accurate map of the earth structure [1, 4-26]. One way to perform seismic imaging is through a technique called wavefield extrapolation [1-5, 27-31]. There exist various extrapolation methods and among them is the so called explicit depth wavefield extrapolation (referred afterwards as wavefield extrapolation) [19, 20, 32-34]. This extrapolation method uses finite impulse response (FIR) filters (named afterwards as extrapolators) that require specific design characteristics. Seismic imaging quality depends upon robust imaging process and thereby on the quality

of the designed FIR wavefield extrapolation filters. This method relies on the assumption that the earth is an acoustic media. It can be used to image two-dimensional(2-D) data sets using one-dimensional(1-D) filters. It can also be used to image three-dimensional(3-D) seismic data sets but with the use of 2-D FIR extrapolation filters [3, 35, 36]. The main goal of this research work is to design 1-D FIR wavefield extrapolation filters, to image 2-D seismic reflection data, with efficient computational design time that can accommodate higher seismic wavefield propagating angles with small passband error, and leads to stable seismic images. The imaging process can be described in the following terms:

- Recording the upward traveling waves at the earth surface.
- Using the recorded waves as initial conditions for the wavefield governed by the wave-equation and, thus, propagating the wave backward using wavefield extrapolation filters in reverse time to the reflector locations.

1.2 Thesis Contributions

In this thesis, it will be shown that the problem of designing such filters can be described and solved using Linear Complementarity problem (LCP). Additionally, such extrapolation filters can be designed via L_1 error approximation. These designed filters are shown to provide stable seismic images with comparable, if not slightly better, seismic imaging results. Both proposed design techniques show efficient designs. These filters are used to extrapolate the 2-D benchmark synthetic

seismic data set known as the Society of Extrapolation Geophysicists/European Association of Geoscientists and Engineers(SEG/EAGE) salt model [4] .

1.3 Thesis Organization

This thesis is organized as follows: chapter 2, describes seismic imaging as a filtering process. In chapter 3, the design problem is formulated via LCP. In chapter 4, L_1 error approximation in the context of FIR wavefield extrapolation filter will be shown. Finally the topic is concluded with the future work suggestions in chapter 5.

CHAPTER 2

SEISMIC IMAGING AS A FILTERING PROCESS

2.1 Introduction

Seismic imaging is the end result of the explicit depth extrapolation process in which the recorded seismic signal at the earth surface $u(x, t, z = 0)$ is propagated back in reverse time to its reflector locations [2,3,27]. Explicit depth extrapolation is attractive due to its computational simplicity and efficiency. One of the advantage of this technique is its explicit filtering that resembles convolution [2, 27, 34] and can be implemented efficiently. In explicit depth extrapolation, short length FIR extrapolation filters are desirable to avoid strong lateral velocity variations in a heterogeneous media while, on the other hand, long FIR extrapolation filters are required to yield accurate extrapolation by accommodating higher propagating angles. Since explicit extrapolators are used recursively in extrapolation process,

the challenge is to design short length FIR extrapolation filter that can cover wider propagating angles while keeping the passband error as small as possible. To understand seismic imaging as a filtering process, it would be interesting to analyze the wavefield governed by wave equation to find origin of such filters.

2.2 One-dimensional extrapolation filters

Assuming that the earth is two-dimensional(2-D) and modeled as an acoustic medium, we can describe the propagating wavefield $u(x, t, z)$ using the following hyperbolic wave equation [1, 32]:

$$\frac{\partial^2 u}{\partial x^2} + \frac{\partial^2 u}{\partial z^2} = \frac{1}{c^2} \frac{\partial^2 u}{\partial t^2}, \quad (2.1)$$

where t represents the time variable, z denotes the depth axis, x is the lateral spatial axis and c is the average velocity.

The 2-D Fourier transform of the wavefield $u(x, t, z)$ with respect to x and t is given by [3]:

$$U(K_x, \Omega_t, z) = \int_{-\infty}^{\infty} \int_{-\infty}^{\infty} u(x, t, z) e^{j(K_x x - \Omega_t t)} dx dt, \quad (2.2)$$

where K_x and Ω_t are the analog wavenumber and angular frequency, respectively.

In light of (2.2), the Fourier transform of the wave equation in (2.1) will produce:

$$\frac{\partial^2 U(K_x, \Omega_t, z)}{\partial z^2} + \left(\frac{\Omega_t^2}{c^2} - K_x^2 \right) U(K_x, \Omega_t, z) = 0, \quad (2.3)$$

where equation (2.3) is a second order homogeneous differential equation. It has a well known solution given by:

$$U(K_x, \Omega_t, z) = A e^{jz\sqrt{\frac{\Omega_t^2}{c^2} - K_x^2}} + B e^{-jz\sqrt{\frac{\Omega_t^2}{c^2} - K_x^2}}. \quad (2.4)$$

The positive exponent refers to an upgoing propagation wavefield while the negative exponent refers to a downward propagation wavefield. Only the upward traveling wavefield is considered here, hence, the solution coefficient B of the downgoing wavefield is set to zero, i.e., $B = 0$. Hence (2.4) becomes:

$$U(K_x, \Omega_t, z) = A e^{jz\sqrt{\frac{\Omega_t^2}{c^2} - K_x^2}}. \quad (2.5)$$

To determine the coefficient A of the upward traveling wavefield, the inverse Fourier transform of $U(K_x, \Omega_t, z)$ is:

$$u(x, t, z) = \int_{-\infty}^{\infty} \int_{-\infty}^{\infty} U(K_x, \Omega_t, z) e^{j(K_x x + \Omega_t t)} dK_x d\Omega_t, \quad (2.6)$$

where (2.5) yields:

$$u(x, t, z) = \int_{-\infty}^{\infty} \int_{-\infty}^{\infty} A e^{jz\sqrt{\frac{\Omega_t^2}{c^2} - K_x^2}} e^{j(K_x x + \Omega_t t)} dK_x d\Omega_t. \quad (2.7)$$

Comparing (2.6) and (2.7) at $z = 0$ yields:

$$A = U(K_x, \Omega_t, 0). \quad (2.8)$$

Equation (2.8) shows that initial condition for solving (2.1) is simply the seismic wavefield recorded at depth $z = 0$, i.e, $u(x, t, z = 0)$ which is what is recorded in the field. Thus, given the initial conditions at $z = z_o$, the wavefield can be extrapolated from depth $z = z_o$ to depth $z = z_o + \Delta z$, where Δz is the depth sampling interval, using the following equation:

$$U(K_x, \Omega_t, z_o + \Delta z) = \begin{cases} U(K_x, \Omega_t, z_o) e^{jz \sqrt{\frac{\Omega_t^2}{c^2} - K_x^2}} & \text{if } |\Omega_t| > c|K_x| \\ \text{or} \\ U(K_x, \Omega_t, z_o) e^{-z \sqrt{K_x^2 - \frac{\Omega_t^2}{c^2}}} & \text{if } |\Omega_t| \leq c|K_x|. \end{cases} \quad (2.9)$$

It is interesting to observe that (2.9) can be written as:

$$U(K_x, \Omega_t, z_o + \Delta z) = U(K_x, \Omega_t, z_o) H_d(K_x, \Omega_t). \quad (2.10)$$

where:

$$H_d(K_x, \Omega_t) = \begin{cases} e^{jz \sqrt{\frac{\Omega_t^2}{c^2} - K_x^2}} & \text{if } |\Omega_t| > c|K_x| \\ \text{or} \\ e^{-z \sqrt{K_x^2 - \frac{\Omega_t^2}{c^2}}} & \text{if } |\Omega_t| \leq c|K_x|. \end{cases} \quad (2.11)$$

$H_d(K_x, \Omega_t)$ is known as the seismic frequency-wavenumber depth extrapolator.

This is a 2-D filter in the $(\Omega - K_x)$ domain where it shows a complex-valued function with a passband $\frac{|\Omega_t|}{c} > K_x$, while in the stopband it is simply a real exponentially decaying function. Figure 2.1 shows the $\Omega - K_x$ response of an ideal 2-D extrapolation filter. In practice, the wavefield is presented in sampled form, so by defining Δt as the temporal sampling, Δx as the horizontal spatial

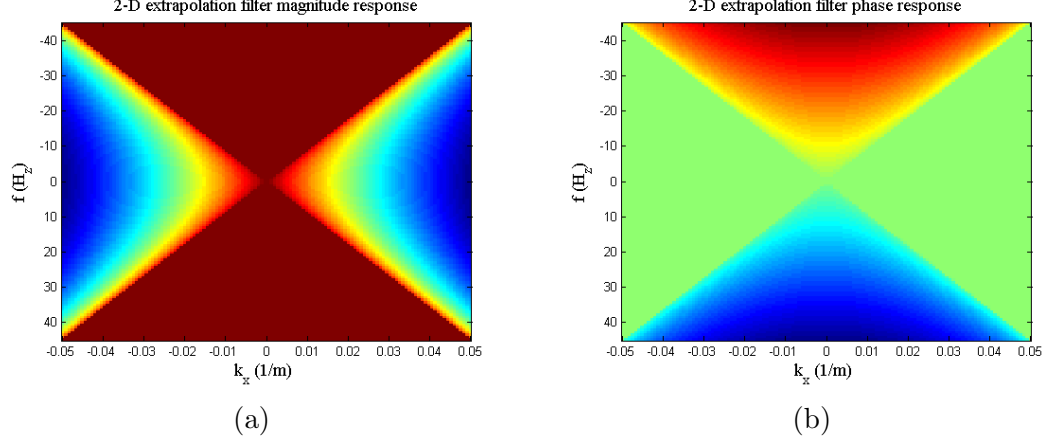


Figure 2.1: (a) Magnitude response of the desired 2-D extrapolation filter, and (b) phase response of the desired 2-D extrapolation filter

sampling, Δz as the depth sampling interval, k_x as the digital wavenumber counterpart of K_x and ω as the digital angular frequency counterpart of Ω_t , the extrapolation operation is carried out using digital filter whose frequency wavenumber $(\omega - k_x)$ response is given by:

$$H_d(e^{jk_x}, e^{j\omega}) = e^{j\frac{\Delta z}{\Delta x} \sqrt{\frac{\Delta x^2}{\Delta t^2} \frac{\omega^2}{c^2} - k_x^2}}. \quad (2.12)$$

The ideal frequency-wavenumber response given by (2.12) corresponds to an all-pass filter. For a single angular frequency ω_o , it becomes a 1-D filter given by:

$$H_d(e^{jk_x}) = e^{j\frac{\Delta z}{\Delta x} \sqrt{\frac{\Delta x^2}{\Delta t^2} \frac{\omega_o^2}{c^2} - k_x^2}} = e^{jb\sqrt{k_c^2 - k_x^2}}, \quad (2.13)$$

where $b = \frac{\Delta z}{\Delta x}$ and $k_c = \frac{\Delta x}{\Delta t} \frac{\Delta \omega}{c}$. As shown in figure 2.2, $H_d(e^{jk_x})$ is a complex valued function with even symmetry, which can be realized by a non-causal FIR digital filter with complex valued impulse response $h[n]$ of even symmetry. Hence,

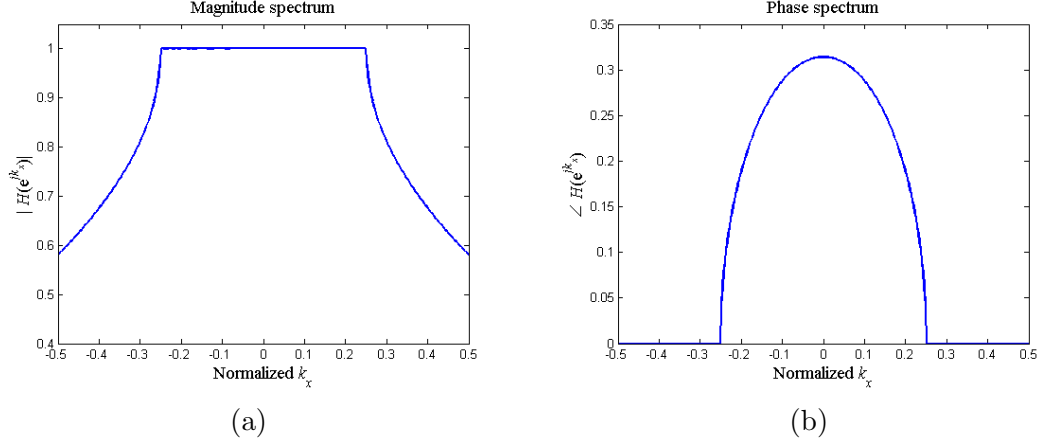


Figure 2.2: (a) Magnitude and (b) phase response of the ideal 1-D extrapolation filter

the wavenumber response of a wavefield extrapolation 1-D FIR filter can be written as (2.14) [3, 28]:

$$H(e^{jk_x}) = \sum_{n=0}^{\frac{N+1}{2}} (2 - \delta[n])h[n] \cos(nk_x). \quad (2.14)$$

These FIR filters are used to obtain seismic images based on extrapolation of seismic wavefields from a depth step to another, where the velocities of the subsurface layers vary vertically but more importantly horizontally.

Such extrapolation filters are frequency-velocity dependent, thus to take care of lateral velocity variations, depth extrapolation is done in the spatial domain by convolving a seismic wavefield with a set of pre-designed FIR extrapolation filters. At the same time, this puts a constraint that the length of the FIR filter should be as small as possible, when the subsurface material varies strongly in the lateral direction. This will additionally maintain a low complexity implementation cost, which in turn imposes a problem of obtaining FIR extrapolation filters with high passband wavenumber response errors that can cause the extrapolation process

to be unstable. These design challenges require novel and robust filter design techniques.

2.3 Subsurface Image

Without loss of generality, in this work, the proposed designs of the FIR extrapolation filters are going to be tested to perform post stack explicit depth $w - x$ extrapolation. First depending on data attributes that is, frequency and velocity, a set of 1-D FIR extrapolation filters will be designed and stored in a lookup table. For each designed 1-D FIR filter, half of the coefficients of such filters are stored due to even symmetry. The explicit depth $w - x$ post stack extrapolation algorithm can be described as follows [1, 3, 5, 31, 32]:

1. Given a stacked seismic data (the wavefield) $u(t, x, z = 0)$, Fourier transform it with respect to t to obtain $U(w, x, z = 0)$.
2. At certain depth interval z_o (starting from $z = 0$), select the first frequency sample and corresponding velocity value.
3. Calculate the filter cutoff k_c , depending on frequency-velocity value, select the proper predesigned extrapolation filter form the look-up table.
4. Perform convolution at the current depth to move to the next depth interval $z = z_o + \Delta z$.
5. Repeat the process for all frequency values.

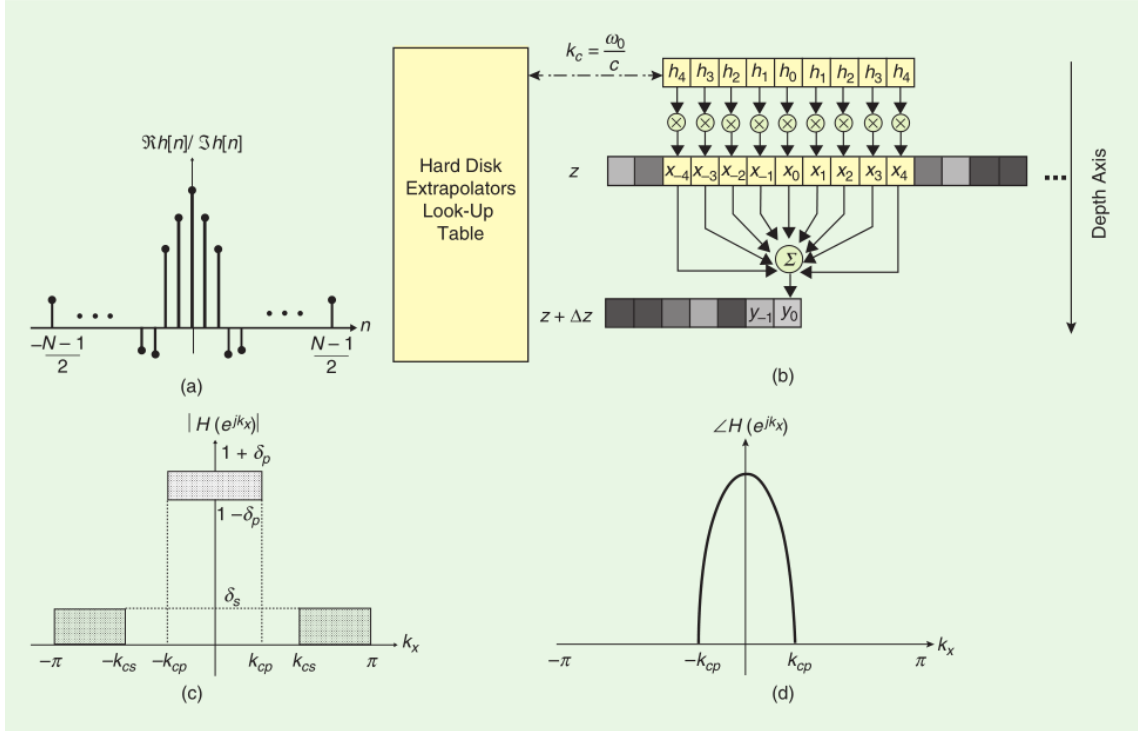


Figure 2.3: Example of a 1-D FIR $w - x$ extrapolation filter requirements. (a) A noncausal spatial impulse response (operator) with even symmetry and (b) a short-length FIR $w - x$ extrapolation filter coefficients for accuracy. Due to the heterogeneity within a layer, the velocity can also vary horizontally. At every lateral position, a new filter is used to perform extrapolation on the data from one depth level to another one. Within the filter length, the medium is assumed to be homogeneous. (c) Accurate magnitude wavenumber response and (d) an accurate passband phase response [1].

6. Iterate the extrapolation algorithm for all depth intervals

After applying the extrapolation algorithm to the maximum depth, sum across frequencies to generate final subsurface image. This process is called the *imaging principle* [1, 3, 5, 31, 32]. For the very first time, Holdberg [27] in 1988, introduced explicit depth extrapolation and since then the problem became a filter design problem. Figure 2.3 summarizes the design requirements of the 1-D FIR extrapolation filter and depth extrapolation process. Performance of seismic extrapolation filter designed by any technique can be judged based on: a) the length of FIR

extrapolation filter, *b*) error in magnitude passband, *c*) accommodation of higher propagating angles in the wavenumber response of small extrapolation filters, and finally, *d*) the phase error in the passband . There exist many techniques [1–5,27–31] to design such filters that offer certain advantages and disadvantages over one another.

In 1988, Holberg [27], who introduced the explicit depth $w - x$ extrapolation technique based on FIR filters, describes a least-squares method for designing explicit wavefield extrapolation filters. These designed filters can lead to unstable extrapolation processes.

FIR wavefield extrapolation filters can be designed by using Taylor series method [32]. In this approach, coefficients of an FIR extrapolator can be realized by comparing N coefficients of the FIR filter with N terms of the Taylor series approximation of Fourier transform of the desired filter. The resultant extrapolation filters tends to be unstable since wavefield energy grows uncontrollably during the extrapolation process [1, 3, 32]. In 1991, Hale [2], proposed a modification of the Taylor series method to produce stable seismic images. He introduced the idea that for extrapolator with N number of coefficients, only $N - p$ coefficients are matched with Taylor series approximation of the desired filter's Fourier transform and remaining p degree of freedom should be used to force amplitude response to zero especially in evanescent region. Though the resultant extrapolator will always result in stable images, however, it cannot accommodate higher propagating

angles, since it attenuates higher wavenumbers. Hence, a large number of coefficients are required to accommodate wavefields with higher propagating angles, which in turn degrade the performance in an inhomogeneous medium.

Karam et.al [28] suggested to design of complex-valued filters, such as 1-D wavefield extrapolation filters, using an extended version of the Park-McClellan algorithm [37]. Under certain conditions, the designed filters will be optimal in the min-max sense for the set of extremal points. If not, it will be optimal with respect to a subset of the whole defined set of extremal points. The optimal design algorithm proved to be efficient in terms of memory and speed of convergence and can result in equiripple responses. However, the FIR wavefield extrapolation filter designed by this method can introduce numerical artifacts in migrated sections and could lead to unstable images [1, 28].

In [29], the author showed that weighted least square optimization technique with smoothed model functions is capable to produce FIR wavefield extrapolation filters that lead into practically stable seismic images. Such an optimization method lacks simplicity as well as requires matrix inversion.

Mousa et.al [3] used projection onto convex sets (POCS) to design FIR extrapolation operators. FIR extrapolation filters designed by this techniques satisfy all designed constraints but the design algorithm is computationally very costly. A modified version of POCS (called MPOCS) was proposed to further reduce the design time and further enhance the wavenumber responses. The designed fil-

ters [3] were applied to the challenging 2-D SEG/EAGE synthetic data [4] and resulted in stable image of the data with a computational cost reduction of 80%, when compared with the most expensive and accurate seismic imaging technique, namely, the phase shift plus interpolation [1, 3, 31].

In an attempt to reduce the implementation cost, sparse FIR extrapolation filters were recently introduced by Mousa [5]. The design relies on further modifying the work in [31] to zero out very small filter coefficients. In addition, an effort to reduce the implementation cost by designing sparse FIR extrapolation filters, the author [31] proved that such filters are not naturally sparse. In [5], author formulated the design problem via L_1 norm and then zero out the coefficients with smaller magnitudes. Designed sparse extrapolators were used to image the data based on the SEG/EAGE salt velocity model. Simulation results showed that proposed algorithm is almost as accurate as PSPI while at the same time reducing the implementation cost.

2.4 Summary

In this chapter, the origin of seismic wavefield extrapolation filters described, assuming that earth is a 2-D acoustic model. The procedure to obtain final subsurface image was discussed, in details, based on the explicit depth $\omega - x$ extrapolation. Next chapter describes mathematical structure of LCP. It will be shown that extrapolation filters can be formulated as a LCP and will result in stable seismic images.

CHAPTER 3

DESIGN OF

ONE-DIMENSIONAL FIR

WAVEFIELD

EXTRAPOLATION FILTER

VIA LINEAR

COMPLIMENTARITY

PROBLEM APPROACH

3.1 Introduction

As stated in Chapter 2, there exist several techniques to design FIR extrapolation filters such as those listed in [1–5, 27–31]. The need to obtain more accurate images of the subsurface requires additional investigation of the techniques and methodologies to design such FIR filters. In this chapter, an alternative new way of designing FIR extrapolation filters is introduced, where the problem will be formulated as a Linear Complementarity Problem (LCP). LCP is not an optimization technique but it unifies the linear and quadratic programs as well as bi-matrix games [38–42]. It will be shown that FIR extrapolation filters can be designed via LCP in the context of Quadratic Programming. There exist mainly two families of algorithms available to solve LCP: *a)* direct (pivoting based) *b)* indirect (iterative) methods [38, 39, 43–50]. The mathematical literature indicates that the LCP can be found as early as 1940 [39]. It has also been called the “composite problem”, the “Fundamental Problem” and the “Complementary Pivot problem” [39]. Cottle proposed the current name “Linear Complementarity Problem” in 1965 [39]. Applications of the LCP theory exist in many fields including Engineering, Economics, etc [38, 39]. For the first time, LCP had been explicitly stated by Du Val in 1940 [39]. His paper, part of algebraic geometry literature, used a problem of the form (q, M) , where q is a vector and M is a square matrix in n dimensional space, to find the least element of the linear inequality system $q + Mz \geq 0, z \geq 0$. Du Val proved that a unique solution exists when Matrix M has special properties [38, 39].

In the context of quadratic programming, the LCP can be found in Hildreth's work [39], Barankin and Dorfman [38, 39]. The LCP problems also appeared in the paper by Frank and Wolfe [38, 39]. All these papers make use of the classical work by Kuhn and Tucker and the Master's Thesis of Karush [38, 39].

The synthesis of linear programming, quadratic programming and bimatrix games as instances of the "fundamental problem" was presented in Cottle and Dantzig [39]. The LCP in terms of complementary cones is represented by Sainelson, Thrall and Wesler [39]. Murty enlarged the topic of complementary cones significantly in 1972 [38]. Nuseirat [51, 52] tested the performance of LCP in the context of the linear phase FIR filter design problem.

In this work the LCP approach has been extended to the complex phase FIR wave-field extrapolation filter. Lemke (direct method) [38, 39] and Fisher-Newton (indirect method) [43] algorithms are used to solve the resulted LCP. For better understanding of the reader the most robust and computationally efficient the Lemke's algorithm [38, 39] is discussed in detail via homotopy theory (See Appendix Chapter A).

3.2 The design of LCP based FIR extrapolation filters

Recall that the ideal 1-D extrapolation filter (2.2) can be given by:

$$H_d(e^{jk_x}) = e^{jb\sqrt{K_c^2 - k_x^2}}. \quad (3.1)$$

Since $H_d(e^{jk_x})$ is a complex valued symmetric function, it can be realized by a non-causal symmetric FIR filter with complex impulse response $h[n]$. Its wavenumber response can be given by:

$$H(e^{jk_x}) = \sum_{n=0}^{\frac{N-1}{2}} (2 - \delta[n])h[n] \cos(nk_x). \quad (3.2)$$

Equation (3.2) can be written as:

$$H(e^{jk_x}) = \sum_{n=0}^M a(n) \cos(nk_x), \quad (3.3)$$

where:

$$M = \frac{N-1}{2}, \quad N \text{ is odd}$$

$$a(0) = h(0)$$

$$a(n) = 2h(n), \quad n \neq 0.$$

$a(n)$ is complex in nature but LCP only deals in a finite-dimensional real vector space. Thus, LCP can only be applied to the problem given by (3.3) by converting

it into two real approximation problems such as:

$$\begin{aligned}
H(e^{jk_x}) &= \sum_{n=0}^M [a_r(n) + ja_i(n)] \cos(nk_x) \\
&= \sum_{n=0}^M a_r(n) \cos(nk_x) + j \sum_{n=0}^M a_i(n) \cos(nk_x) \\
&= H_r(e^{jk_x}) + jH_i(e^{jk_x}).
\end{aligned} \tag{3.4}$$

If $H_d = H_{d_r} + jH_{d_i}$ is the ideal wavenumber response, then $a_r(n)$ and $a_i(n)$ can be recovered by solving:

$$H_l(e^{jk_x}) = \sum_{n=0}^M a_l(n) \cos(nk_x), \quad l = r, i. \tag{3.5}$$

where r and i stands for real and imaginary, respectively. Now, applying wavenumber grid $\{k_{x_p} | 1 \leq p \leq L\}$ (3.5) can be written in the following matrix form:

$$\mathbf{H}_l = \mathbf{C}\mathbf{a}_l, \quad l = r, i, \tag{3.6}$$

where

$$\mathbf{C} = \begin{bmatrix} 1 & \cos(k_{x_1}) & \cdot & \cdot & \cdot & \cos(Mk_{x_1}) \\ \cdot & \cdot & \cdot & \cdot & \cdot & \cdot \\ \cdot & \cdot & \cdot & \cdot & \cdot & \cdot \\ 1 & \cos(k_{x_k}) & \cdot & \cdot & \cdot & \cos(Mk_{x_k}) \\ \cdot & \cdot & \cdot & \cdot & \cdot & \cdot \\ \cdot & \cdot & \cdot & \cdot & \cdot & \cdot \\ \cdot & \cdot & \cdot & \cdot & \cdot & \cdot \\ 1 & \cos(k_{x_L}) & \cdot & \cdot & \cdot & \cos(Mk_{x_L}) \end{bmatrix}, \quad \mathbf{a} = \begin{bmatrix} a(0) \\ a(1) \\ \cdot \\ \cdot \\ \cdot \\ a(M-1) \\ a(M) \end{bmatrix}.$$

Since LCP solves for a vector ≥ 0 , then $\{\mathbf{a}_l, \quad l = r, i\}$ has to be written as a difference of two positive vectors:

$$\begin{aligned} \mathbf{a}_l &= \mathbf{a}_l^+ + \mathbf{a}_l^-, \quad l = r, i \\ \mathbf{a}_l^+ &\geq 0 \\ \mathbf{a}_l^- &\geq 0 \end{aligned} \tag{3.7}$$

Using equation (3.6), $\{\mathbf{H}_l, \quad l = r, i\}$ can be written as:

$$\begin{aligned} \mathbf{H}_l &= \mathbf{C} \begin{bmatrix} \mathbf{a}_l^+ & \mathbf{a}_l^- \end{bmatrix} \\ &= \begin{bmatrix} \mathbf{C} & -\mathbf{C} \end{bmatrix} \begin{bmatrix} \mathbf{a}_l^+ \\ \mathbf{a}_l^- \end{bmatrix} \\ &= \mathbf{B}\mathbf{x}_l, \quad l = r, i, \end{aligned} \tag{3.8}$$

where

$$\mathbf{B} = \begin{bmatrix} \mathbf{C} & -\mathbf{C} \end{bmatrix}, \quad \mathbf{x} = \begin{bmatrix} \mathbf{a}_l^+ \\ \mathbf{a}_l^+ \end{bmatrix}.$$

Since $\mathbf{H}_d = \mathbf{H}_{d_r} + j\mathbf{H}_{d_i}$ is the ideal wavenumber response, thus the error vector $\{\mathbf{E}_l, \quad l = r, i\}$ will be

$$\mathbf{E}_l = \mathbf{B}\mathbf{x}_l - \mathbf{H}_{d_l}, \quad l = r, i. \quad (3.9)$$

The problem of finding $\{\mathbf{a}_l, \quad l = r, i\}$ can be formulated by minimizing the squared error:

$$\begin{aligned} &\text{Minimize } \varepsilon(\mathbf{x}_l) = \mathbf{E}_l^T \mathbf{E}_l \\ &\text{Subject to} \end{aligned} \quad (3.10)$$

$$|\mathbf{E}_l| \leq \delta, \quad l = r, i,$$

where δ is the tolerance scheme. The objective function in (3.10) can be written as:

$$\begin{aligned} \varepsilon(\mathbf{x}_l) &= \mathbf{E}_l^T \mathbf{E}_l, \\ &= (\mathbf{B}\mathbf{x}_l - \mathbf{H}_{d_l})^T (\mathbf{B}\mathbf{x}_l - \mathbf{H}_{d_l}), \\ &= (\mathbf{x}_l^T \mathbf{B}^T - \mathbf{H}_{d_l}^T) (\mathbf{B}\mathbf{x}_l - \mathbf{H}_{d_l}), \\ &= \mathbf{x}_l^T \mathbf{B}^T \mathbf{B}\mathbf{x}_l - \mathbf{x}_l^T \mathbf{B}^T \mathbf{H}_{d_l} - \mathbf{H}_{d_l}^T \mathbf{B}\mathbf{x}_l + \mathbf{H}_{d_l}^T \mathbf{H}_{d_l}, \\ &= \mathbf{x}_l^T \mathbf{B}^T \mathbf{B}\mathbf{x}_l - 2\mathbf{x}_l^T \mathbf{B}^T \mathbf{H}_{d_l} + \mathbf{H}_{d_l}^T \mathbf{H}_{d_l}. \\ \varepsilon(\mathbf{x}_l) &= \frac{1}{2} \mathbf{x}_l^T \mathbf{Q}\mathbf{x}_l - \mathbf{x}_l^T \mathbf{R} + \mathbf{H}_{d_l}^T \mathbf{H}_{d_l}, \quad l = r, i, \end{aligned} \quad (3.11)$$

where $\mathbf{x} \in R^{2M+2}$ and $\mathbf{Q} = 2\mathbf{B}^\tau\mathbf{B}$ is symmetric and semi-positive definite matrix,
 $\mathbf{R} = 2\mathbf{B}^\tau\mathbf{H}_{d_l}$.

The linear constraints in problem (3.10) can be written in a compact form as follows

$$\begin{aligned}
|\mathbf{E}_l| &\leq \delta \\
|\mathbf{B}\mathbf{x}_l - \mathbf{H}_d| &\leq \delta \\
\underbrace{\begin{bmatrix} \mathbf{B} \\ -\mathbf{B} \end{bmatrix}}_{\mathbf{A}} \mathbf{x}_l &\leq \underbrace{\begin{bmatrix} \mathbf{H}_d + \delta \\ -\mathbf{H}_d + \delta \end{bmatrix}}_{\mathbf{b}}, \quad l = r, i.
\end{aligned} \tag{3.12}$$

Finally, the minimization problem (3.10) becomes:

$$\begin{aligned}
\text{Minimize } f(\mathbf{x}_l) &= \frac{1}{2}\mathbf{x}_l^\tau\mathbf{Q}\mathbf{x}_l - \mathbf{x}_l^\tau\mathbf{R} + \mathbf{H}_{d_l}^\tau\mathbf{H}_{d_l}, \quad l = r, i \\
\text{Subject to} & \\
\mathbf{A}\mathbf{x}_l &\leq \mathbf{b} \\
\mathbf{x}_l &\geq 0
\end{aligned} \tag{3.13}$$

The Kuhn-Tucker necessary conditions for the above quadratic programs (3.13) (see Appendix Chapter A) are that there must exist vectors $\mathbf{u} \in R^{2M+2}$, $\mathbf{v} \in R^{2L}$, $\lambda \in R^{2L}$ such that:

$$\begin{aligned}
-\mathbf{R} + \mathbf{Q}\mathbf{x} + \mathbf{A}^\tau\lambda - \mathbf{u} &= 0, \\
\mathbf{A}\mathbf{x} + \mathbf{v} &= \mathbf{b}, \\
\mathbf{u} \geq 0, \mathbf{v} \geq 0, \mathbf{x} \geq 0, \lambda \geq 0, \mathbf{u}^\tau\mathbf{x} &= 0, \mathbf{v}^\tau\lambda = 0.
\end{aligned} \tag{3.14}$$

Clearly, this can be written as:

$$\begin{pmatrix} \mathbf{u} \\ \mathbf{v} \end{pmatrix} \equiv \begin{pmatrix} -\mathbf{R} \\ \mathbf{b} \end{pmatrix} + \begin{pmatrix} \mathbf{Q} & \mathbf{A}^\tau \\ -\mathbf{A} & 0 \end{pmatrix} \begin{pmatrix} \mathbf{x} \\ \lambda \end{pmatrix}, \quad (3.15)$$

$$\mathbf{u} \geq 0, \mathbf{v} \geq 0, \mathbf{x} \geq 0, \lambda \geq 0, \mathbf{u}^\tau \mathbf{x} = 0, \mathbf{v}^\tau \lambda = 0.$$

The minimization problem (3.10) represents a LCP. In a compact form LCP for the problem (3.10) can be written as

$$\begin{aligned} \mathbf{z} - \mathbf{M}\mathbf{w} &= \mathbf{q}, \\ \mathbf{z} \geq 0, \quad \mathbf{w} \geq 0, \quad \mathbf{z}^\tau \mathbf{w} &= 0, \end{aligned} \quad (3.16)$$

where

$$\mathbf{M} = \begin{bmatrix} \mathbf{Q} & \mathbf{A}^\tau \\ -\mathbf{A} & 0 \end{bmatrix}, \quad \mathbf{z} = \begin{bmatrix} \mathbf{y} \\ \mathbf{v} \end{bmatrix}, \quad \mathbf{w} = \begin{bmatrix} \mathbf{x} \\ \mathbf{u} \end{bmatrix}, \quad \mathbf{q} = \begin{bmatrix} -\mathbf{R} \\ \mathbf{b} \end{bmatrix}.$$

If \mathbf{Q} is a semi-definite positive matrix then \mathbf{M} is also a semi-definite positive matrix. Thus, the problem of designing 1-D FIR wavefield extrapolation filter is an example of semi-definite LCP. There are many algorithms available to solve semi-definite LCP including Lemke's algorithm and Fisher-Newton algorithm [38, 39, 43–50]. As stated in [39, 51] that if \mathbf{Q} is positive semi definite and \mathbf{x} is the K-T point of (3.16) then \mathbf{x} is the optimal feasible point of (3.16).

3.2.1 Design Algorithm

1. Select the filter length N , cutoff k_c as well as tolerance scheme δ .
2. Formulate matrices \mathbf{H}_d , \mathbf{B} as well as \mathbf{E} based on equations (3.1), (3.8) and (3.9).
3. Formulate matrices \mathbf{Q} , \mathbf{R} , \mathbf{A} and vector \mathbf{b} according to equations (3.11) and (3.12).
4. Formulat Matrix \mathbf{M} and vector \mathbf{q} based on equation (3.16).
5. Solve the problem (3.16) to get the filter coefficients.

The summary of the proposed, LCP based, algorithm for designing the $f - x$ FIR extrapolation digital filters is shown in figure 3.1.

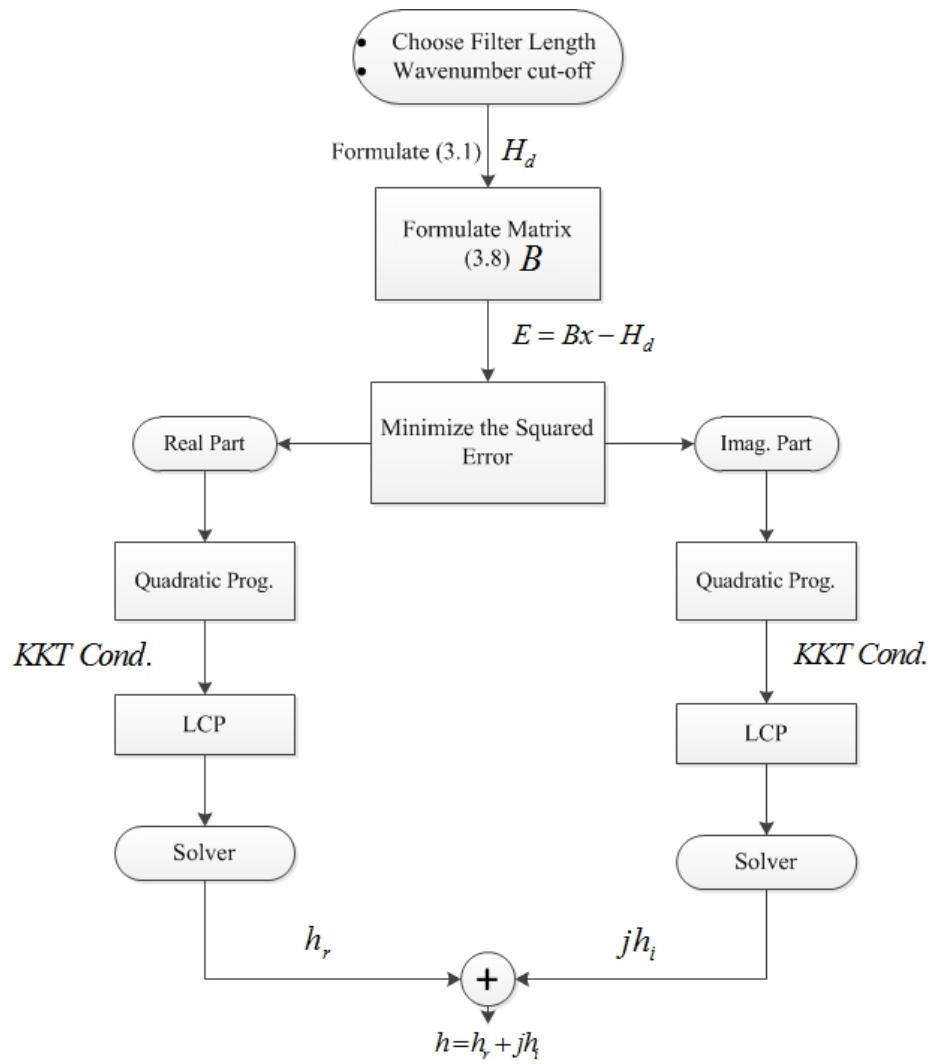


Figure 3.1: LCP based work flow of the algorithm to design $f - x$ FIR wavefield extrapolation filters.

3.3 Simulation Results

In this section, a set of design examples is provided of different 1-D FIR wavefield extrapolation filter for decaying parameter $b = 0.2$, a cutoff, $k_c = 0.25$ and various lengths ($N = 25, 35$). The objective is to show various designs using LCP-Lemke and LCP Fisher-Newton algorithms, the modified Taylor series [2] and MPOCS [3]. Figure 3.2 and 3.3 show the magnitude and phase performance as well as error in passband of an FIR wavefield extrapolation filter with $N = 25$ and $N = 35$ for cutoff $k_c = 0.25$ and decaying parameter $b = 0.2$.

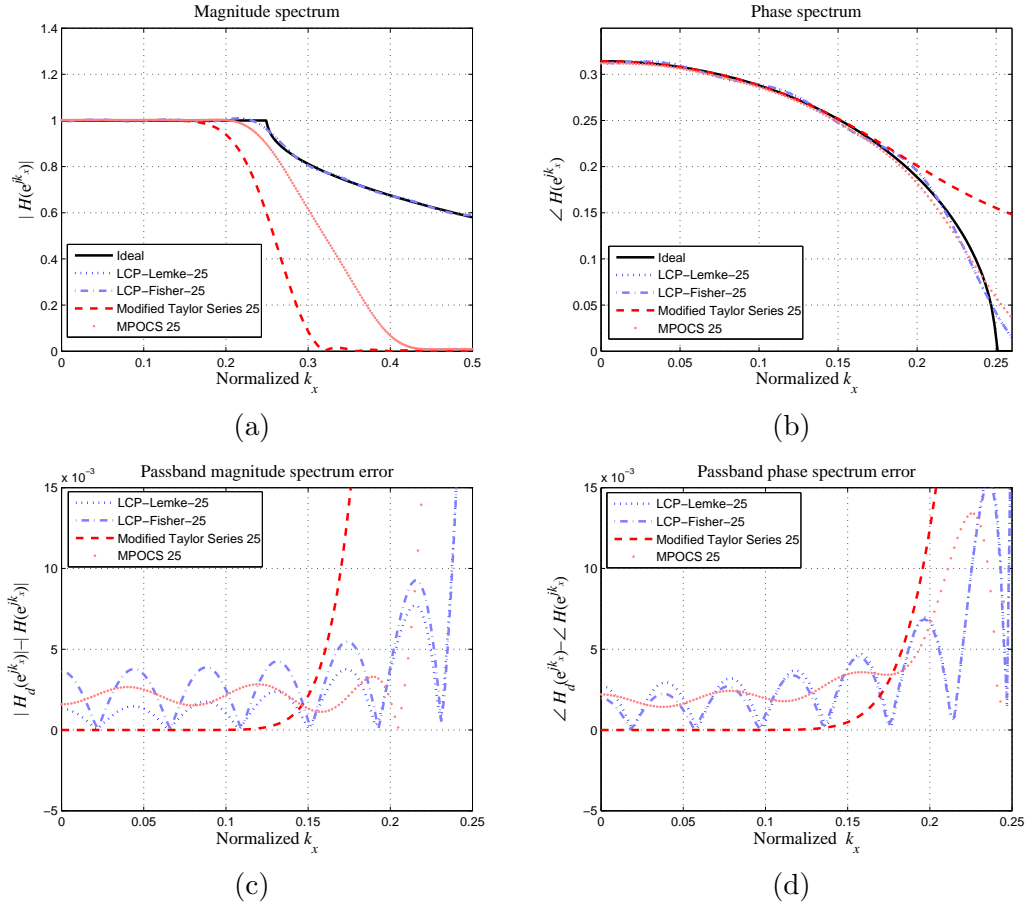


Figure 3.2: (a) Magnitude and (b) phase response of 1-D extrapolation filter designed by LCP-Lemke, LCP-Fisher, the modified Taylor series [2] and MPOCS [3] (c) and (d) show the passband magnitude and phase errors, respectively.

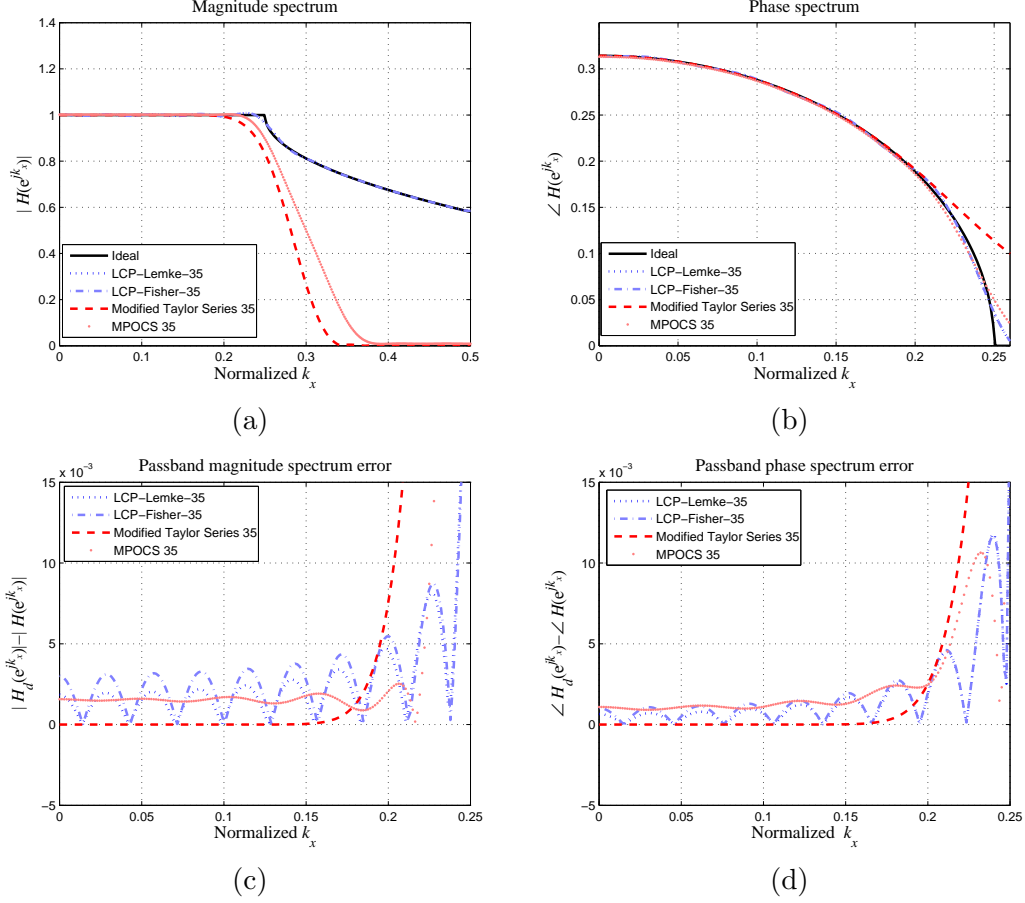


Figure 3.3: (a) Magnitude and (b) phase response of 1-D extrapolation filter designed by LCP-Lemke and LCP-Fisher, the modified Taylor series [2] and MPOCS [3] (c) and (d) show the passband magnitude and phase errors, respectively.

Clearly, such designs will result in stable seismic images, as will be seen in the next section. MPOCS [3] and the modified Taylor series [2] produce small passband error but attenuate wavefields propagating with higher angles. On the other hand, the LCP approach accommodates higher propagating angles and at the same time LCP-Lemke design generally shows less wavenumber errors, when compared to those errors of LCP-Fisher designed filters. This will be reflected on the imaged SEG/EAGE salt data in the next section. In addition, the LCP-

Table 3.1: Comparison of CPU (core-i5) design time for designing 1-D FIR extrapolation filter with 25 and 35 coefficients designed via LCP-Lemke and LCP-Fisher-Newton algorithms

Method	Coefficients	Iterations	CPU design time(<i>s</i>)
LCP-Lemke	25	None	0.062
LCP-Fisher	25	10	1.295
Mod. Taylor Series	25	None	0.869
MPOCS	25	89	0.1872
LCP-Lemke	35	None	0.078
LCP-Fisher	35	10	2.2
Mod. Taylor Series	35	None	2.959
MPOCS	35	85	0.2340

Lemke’s algorithm outperforms Fisher-Newton method, the modified Taylor series [2] and MPOCS [3] in the computational design time. Table 3.1 shows the design computational time for the filters in figure 3.2 and 3.3.

3.4 Application to SEG/EAGE Salt Model

For the purpose of studying the effectiveness of the proposed LCP 1-D FIR extrapolation filters, the famous challenging SEG/EAGE salt velocity model is extrapolated via FIR wavefield extrapolation filters designed by LCP. The SEG/EAGE salt model [4] contains smoothly varying velocities and is composed of 1048 depth samples for 1024 traces each (see figure 3.4). The zero offset section for salt model (see figure 3.5) generated by finite difference method contains 3001 time samples for 1024 traces each [1,4,5]. The sampling parameters for the salt model: $\Delta z = 2m$, $\Delta x = 10m$ and $\Delta t = 0.002s$ and maximum frequency $f_{max} = 45Hz$. To properly extrapolate this zero-offset data, 7000 1-D FIR extrapolation filters are pre-designed and stored in a look-up table. Final subsurface image has been

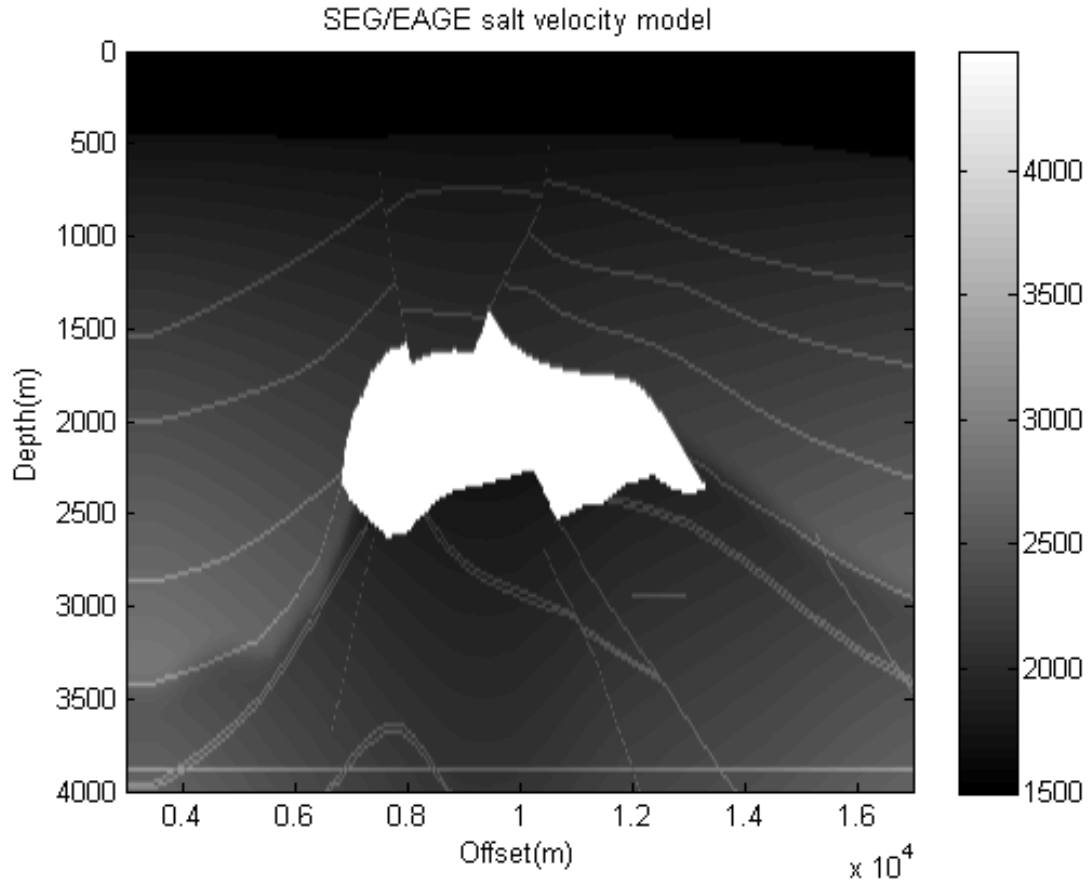


Figure 3.4: Shows the SEG/EAGE salt velocity model. Velocity changes from minimum value 1,500 m/s that correspond to the acoustics speed in water represented by black color to maximum value 4,500 m/s that correspond to the acoustics speed in salt represented by white color.

obtained by following the procedure described in chapter 2.

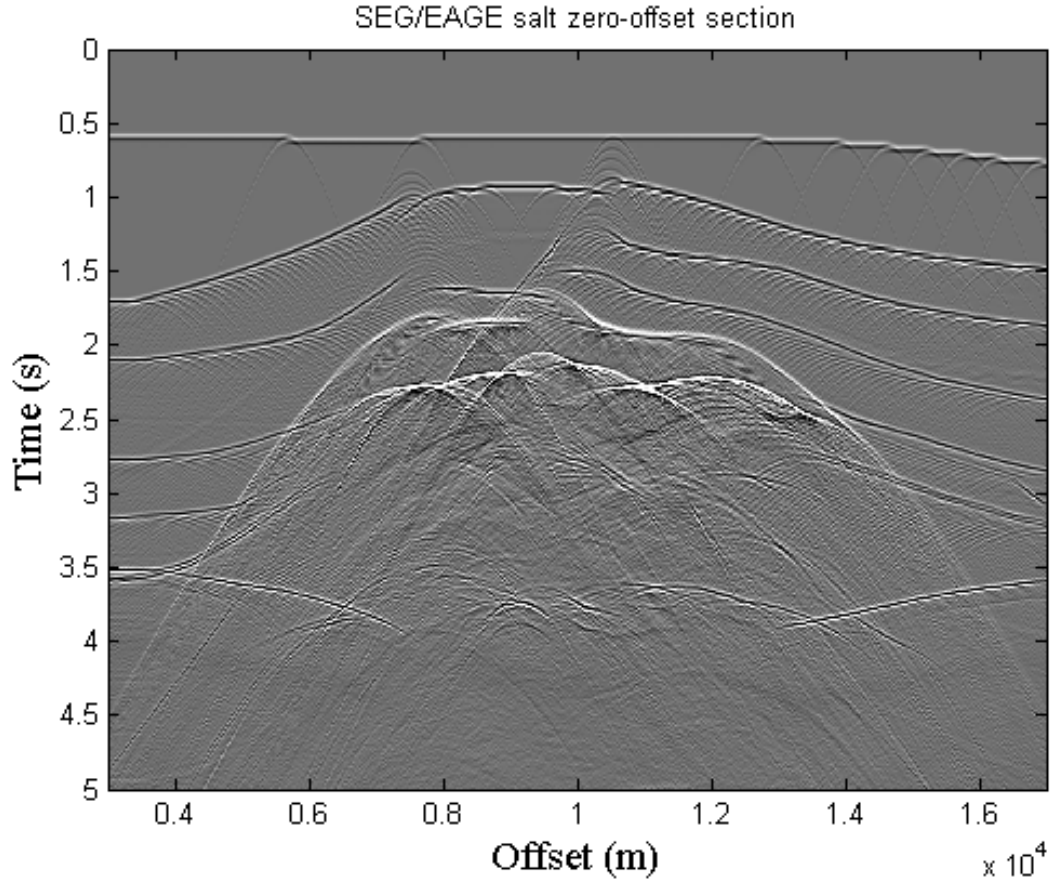


Figure 3.5: Shows the zero-offset section of the SEG/EAGE Salt Model, generated based on finite difference method [4]. Performance of LCP has been tested on this data set.

Figure 3.6 and 3.7 show the wavenumber response of such filters (with 25 and 35 coefficients, respectively) designed via Lemke and Fisher-Newton algorithm. The errors between the wavenumber magnitude and phase responses of extrapolation filters designed via LCP-Lemke and LCP-Fisher algorithms indicate that the extrapolation filters designed via Fisher-Newton algorithm have highpass band magnitudes which will effect the final subsurface image. However, this can be observed that these errors are reduced when N was incresed from 25 to 35.

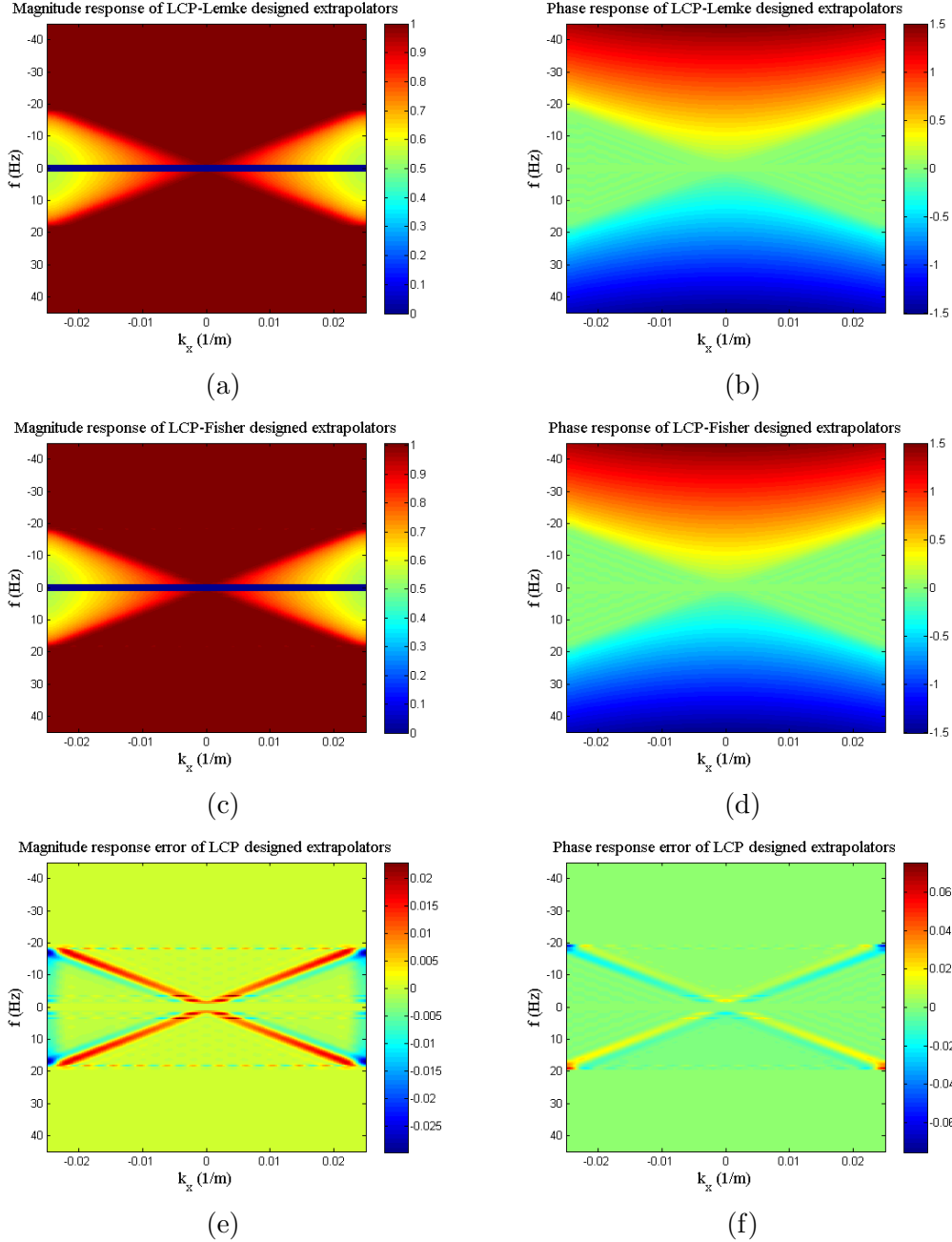


Figure 3.6: Set of designed $f - x$ FIR extrapolation filters in the frequency wavenumber domain with $N = 25$ (a) and (b) show the magnitude and phase responses of Lemke's algorithm, (c) and (d) show the magnitude and phase responses of Fisher's algorithm, (e) and (f) show error between the frequency wavenumber responses for the magnitude and phase responses, respectively.

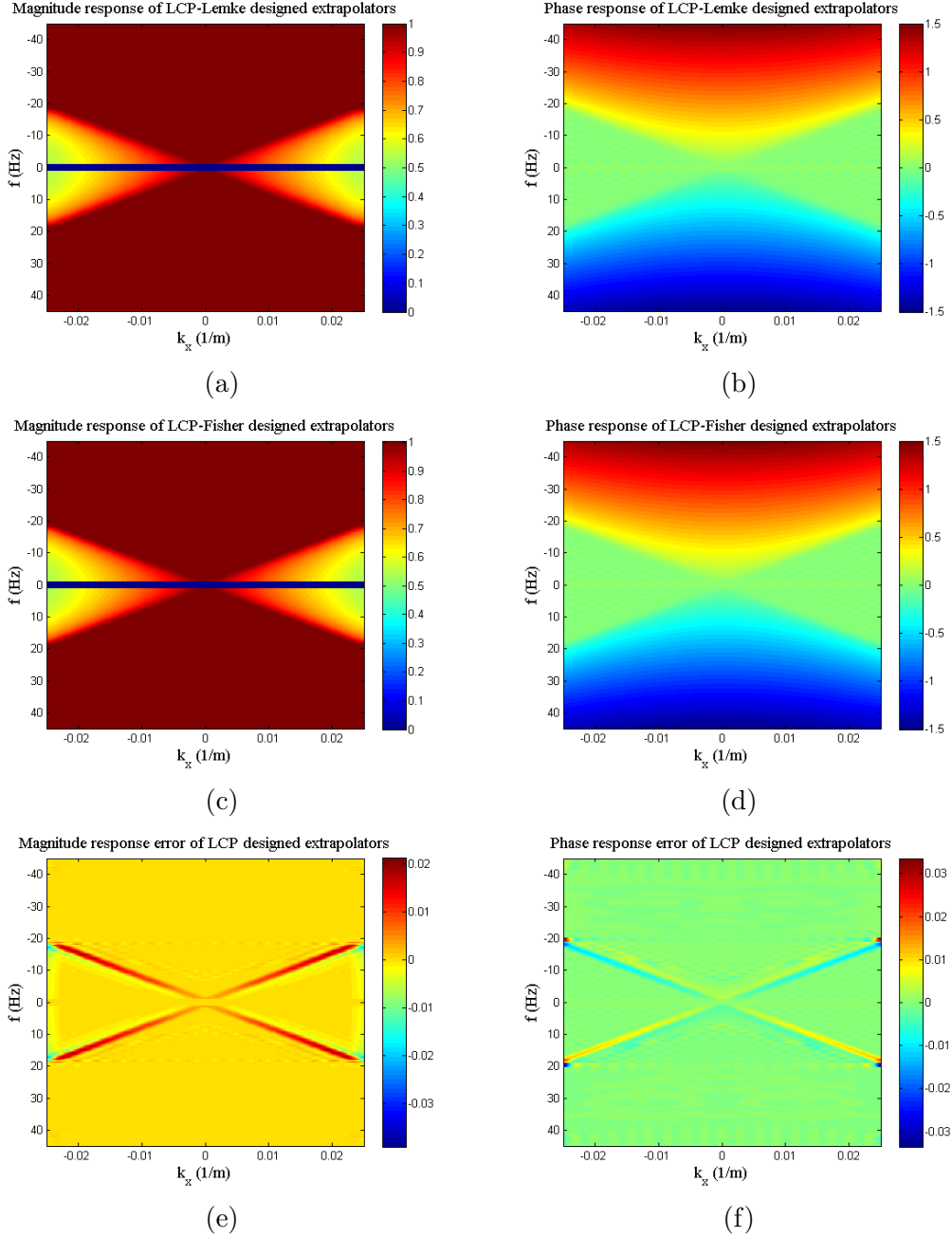


Figure 3.7: Set of designed $f - x$ FIR extrapolation filters in the frequency wavenumber domain with $N = 35$ (a) and (b) show the magnitude and phase responses of Lemke’s algorithm, (c) and (d) show the magnitude and phase responses of Fisher’s algorithm, (e) and (f) show error between the frequency wavenumber responses for the magnitude and phase responses, respectively.

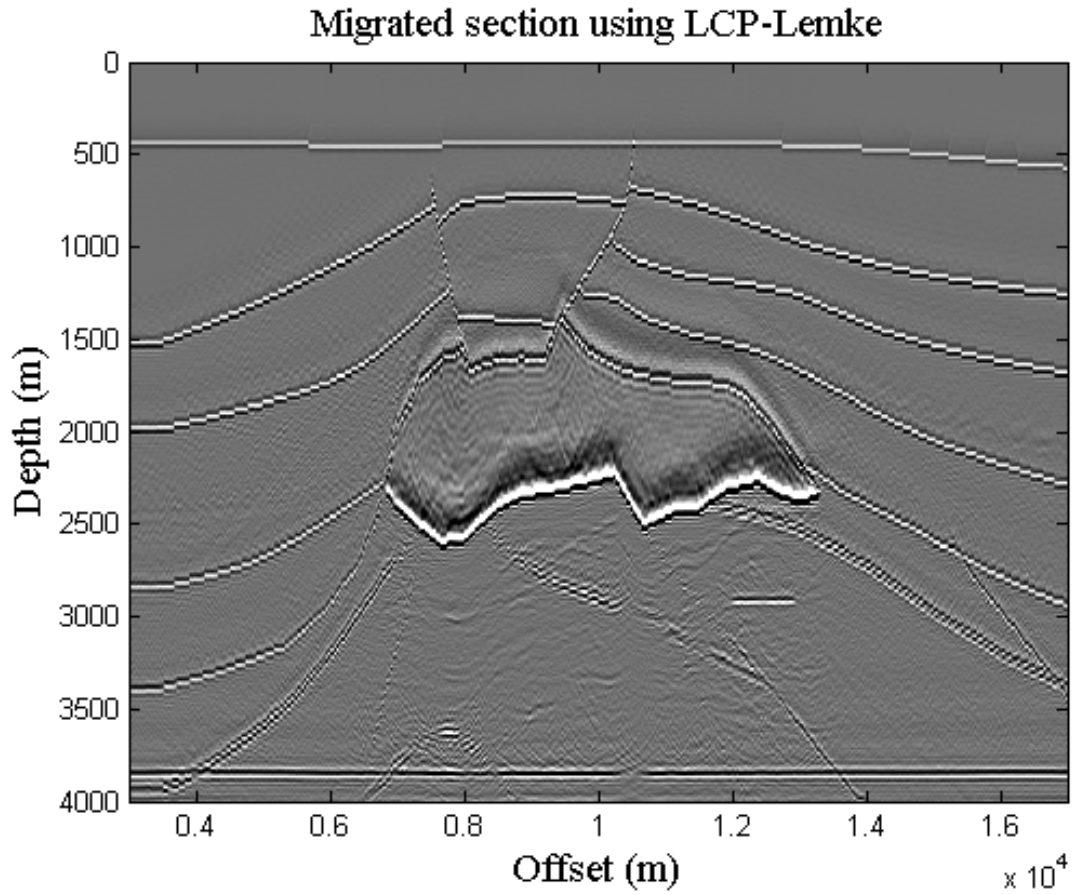


Figure 3.8: Extrapolated SEG/EAGE salt model using Lemke algorithm with 25-coefficients.

Figure 3.8 shows subsurface image that has been produced by extrapolating SEG/EAGE salt velocity model using extrapolation filters with 25-coefficients designed via LCP-Lemke method, whereas figure 3.9 shows the same data extrapolated but with LCP-Fisher-Newton method ($N = 25$)

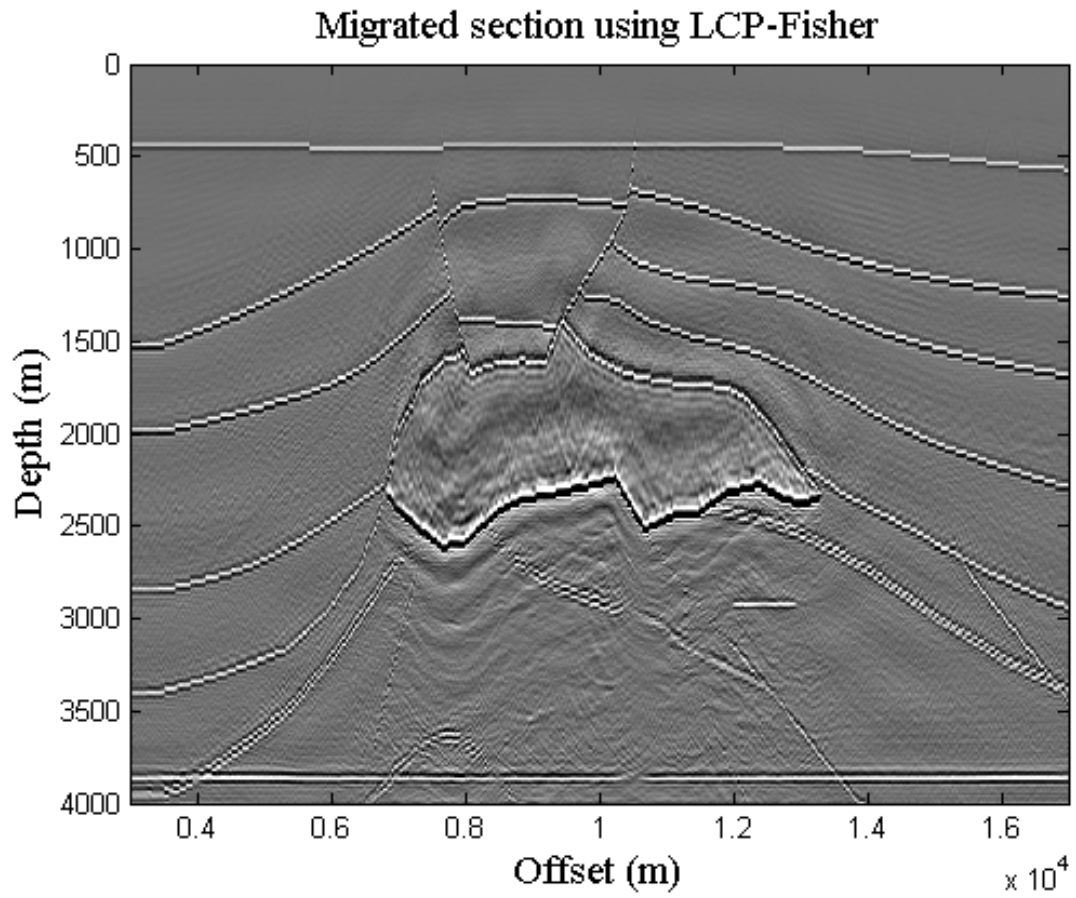


Figure 3.9: Extrapolated SEG/EAGE salt model using Fisher-Newton algorithm with 25-coefficients.

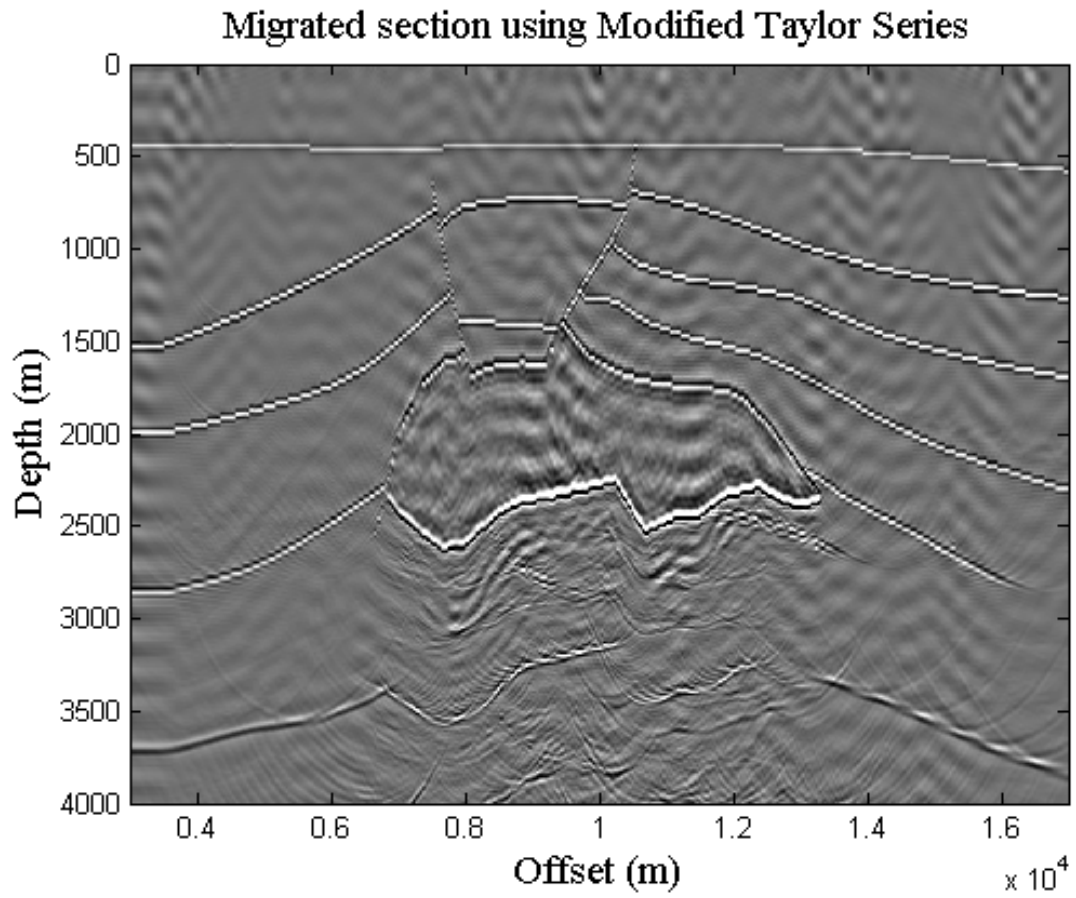


Figure 3.10: Extrapolated SEG/EAGE salt model using Modified Taylor Series [2] with 25-coefficients.

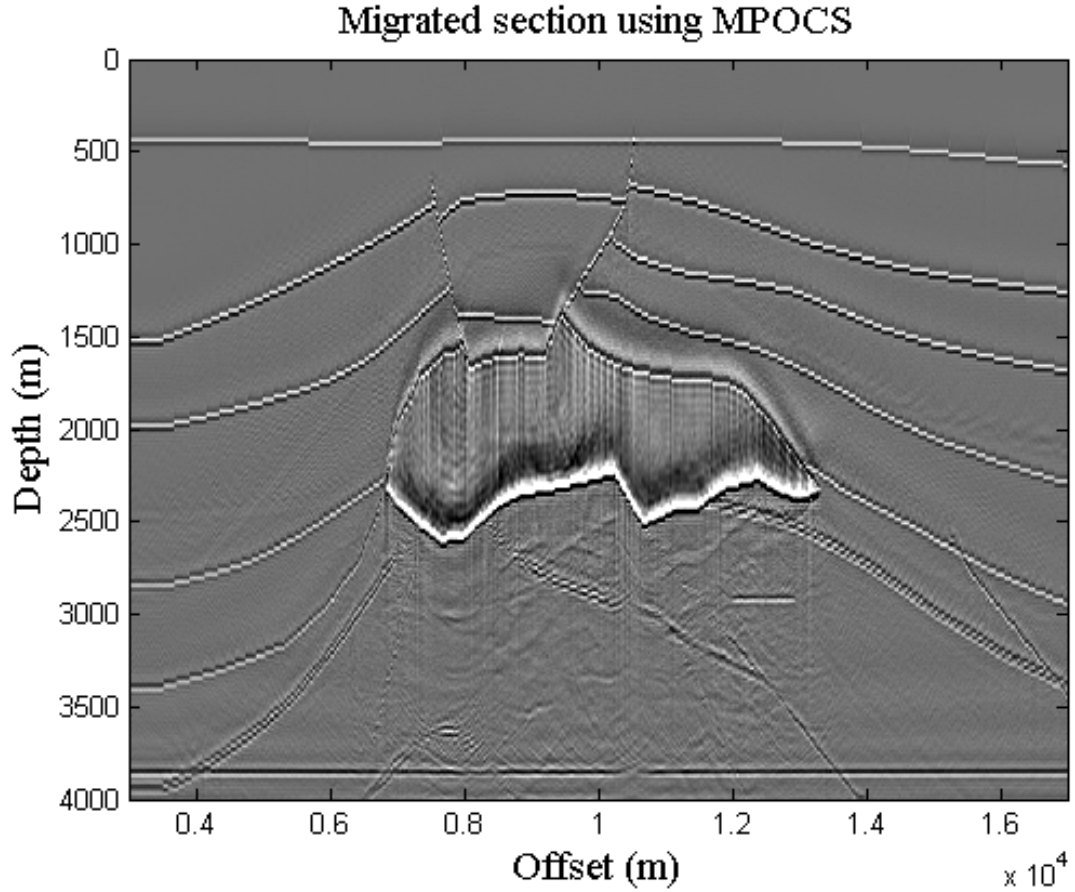


Figure 3.11: Extrapolated SEG/EAGE salt model using Modified Projection Onto Convex Sets (MPOCS) [3] with 25-coefficients.

It can be observed that extrapolation filters designed via the LCP-Lemke algorithm and Fisher-Newton method produce much better subsurface image than the modified Taylor series [2] and modified projection onto convex sets (MPOCS) [3]. Fisher-Newton method produce ghost effects of the salt dome in the final image, due to the high passband wavenumber response of extrapolation filters designed via LCP-Fisher Newton method, when compared with those of the LCP-Lemke ones.

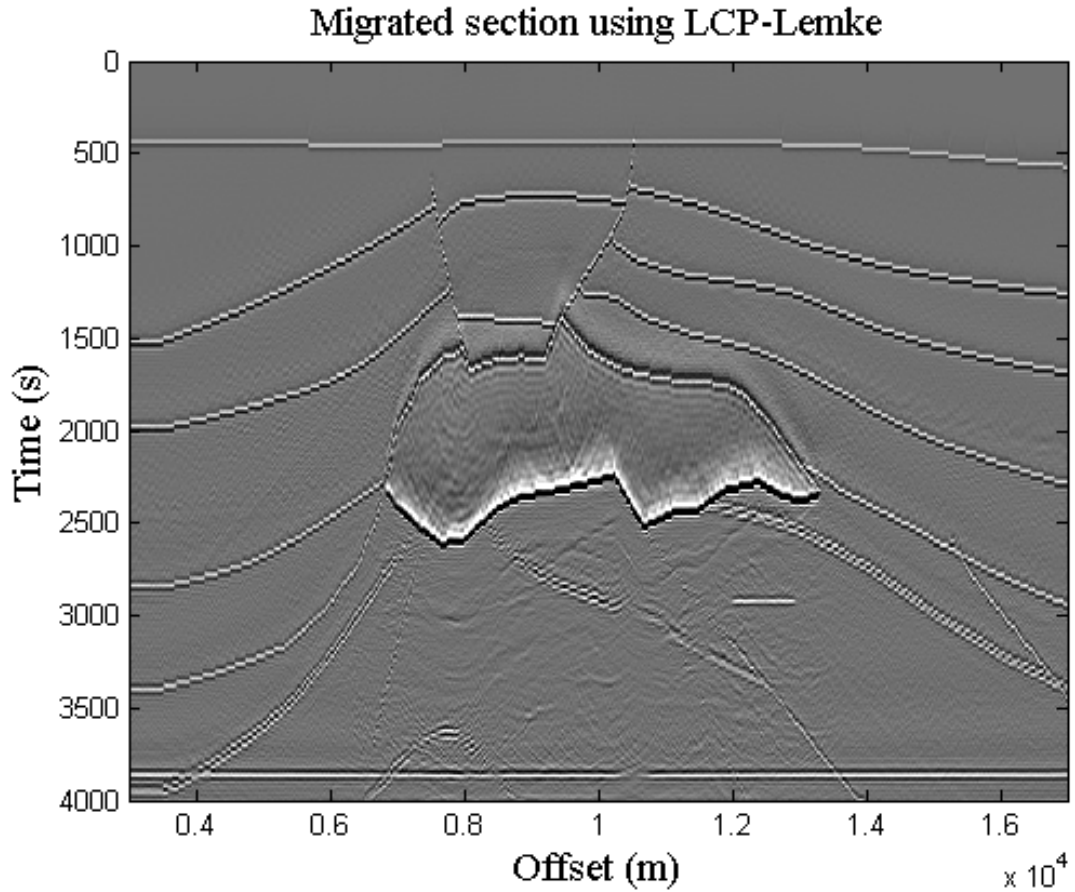


Figure 3.12: Extrapolated SEG/EAGE salt model using Lemke algorithm with 35-coefficients.

Figures 3.12 and 3.13 clearly show that the subsurface images generated by using FIR extrapolation filters with 35 coefficients are of better quality than subsurface images generated by using extrapolation filters with only 25 coefficients. This improvement in quality is because by increasing the number of filter coefficients, the passband wavenumber response errors have decreased.

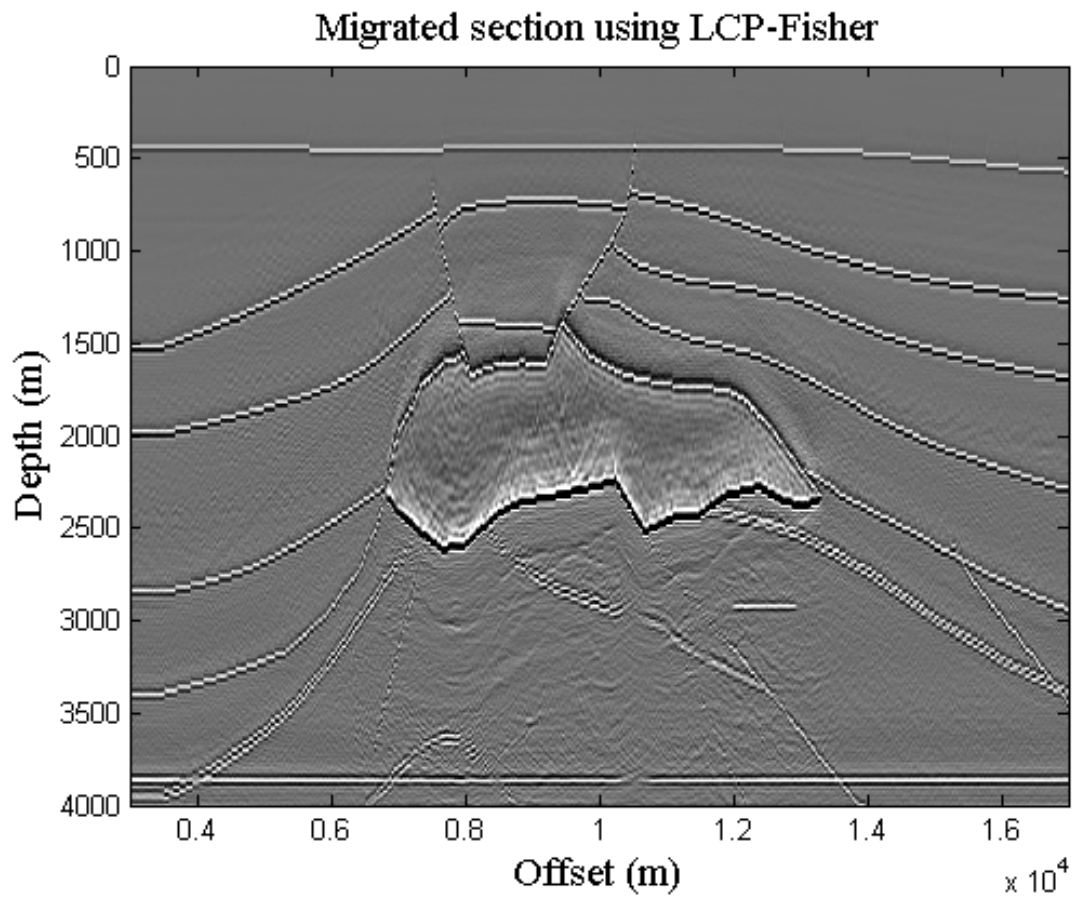


Figure 3.13: Extrapolated SEG/EAGE salt model using Fisher-Newton algorithm with 35-coefficients.

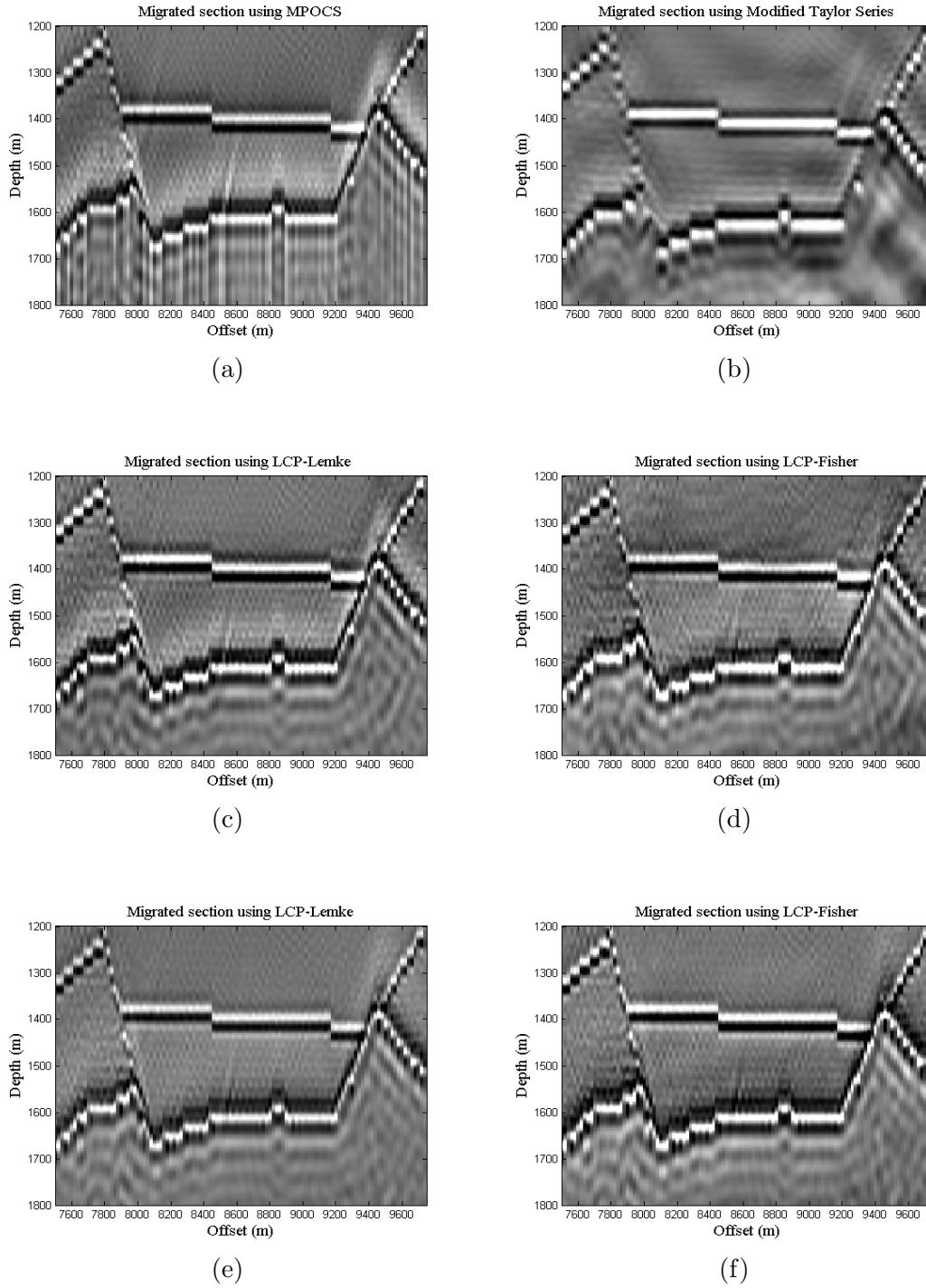


Figure 3.14: Details of an area with different dips (lateral position of 7500–9750m and depth of 1200–1800m) using (a) MPOCS [3] ($N = 25$) (b) Modified Taylor Series [2] ($N = 25$) (c) LCP-Lemke ($N = 25$), (d) LCP-Fisher ($N = 25$), (e) LCP-Lemke ($N = 35$), (f) LCP-Fisher ($N = 35$)

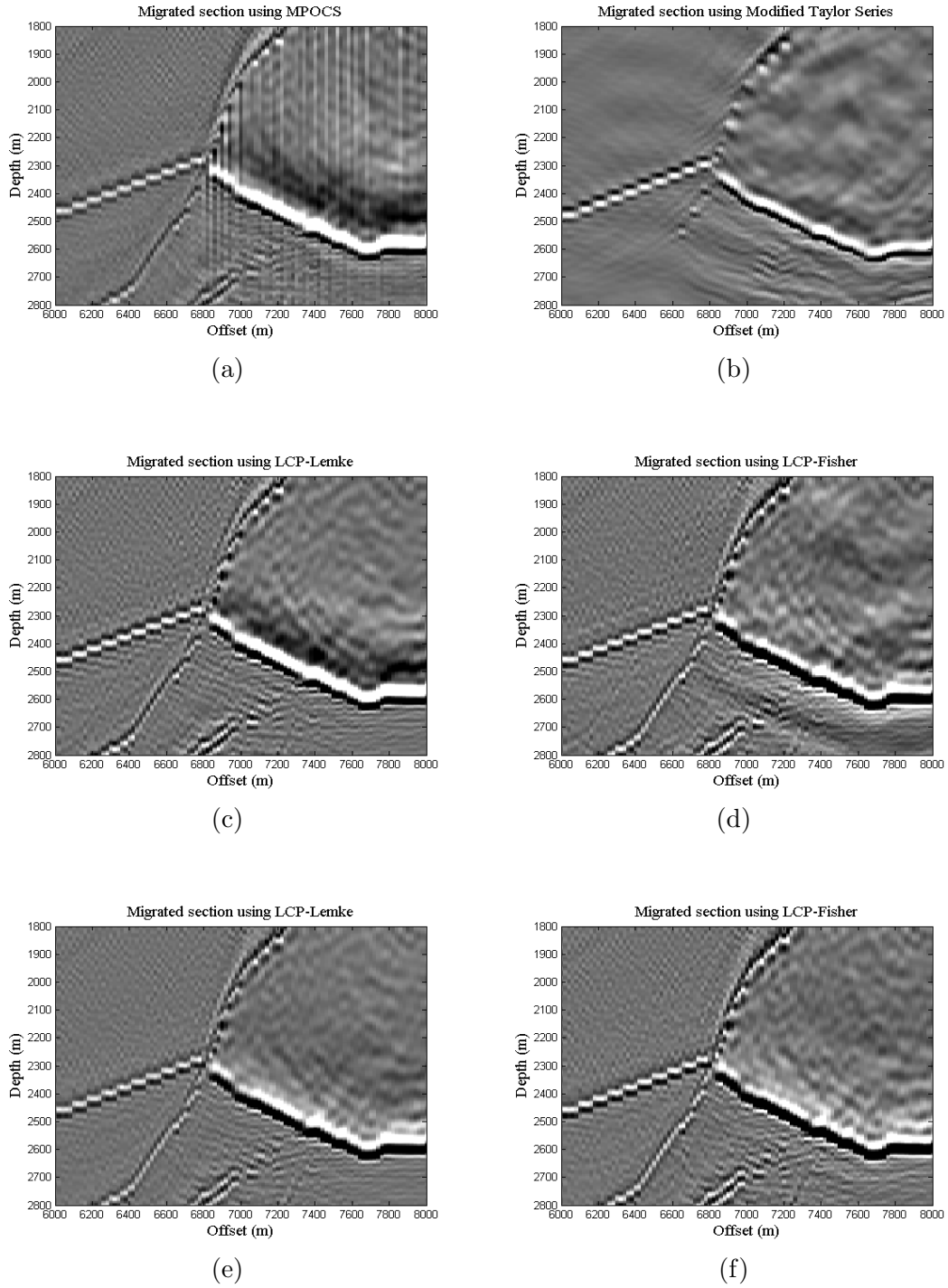


Figure 3.15: Details of an area with step dips on the left flank of the salt model (lateral position of 6000–8000m and depth of 1800–2800m) using (a) MPOCS [3] ($N = 25$) (b) Modified Taylor Series [2] ($N = 25$) (c) LCP-Lemke ($N = 25$), (d) LCP-Fisher ($N = 25$), (e) LCP-Lemke ($N = 35$), (f) LCP-Fisher ($N = 35$)

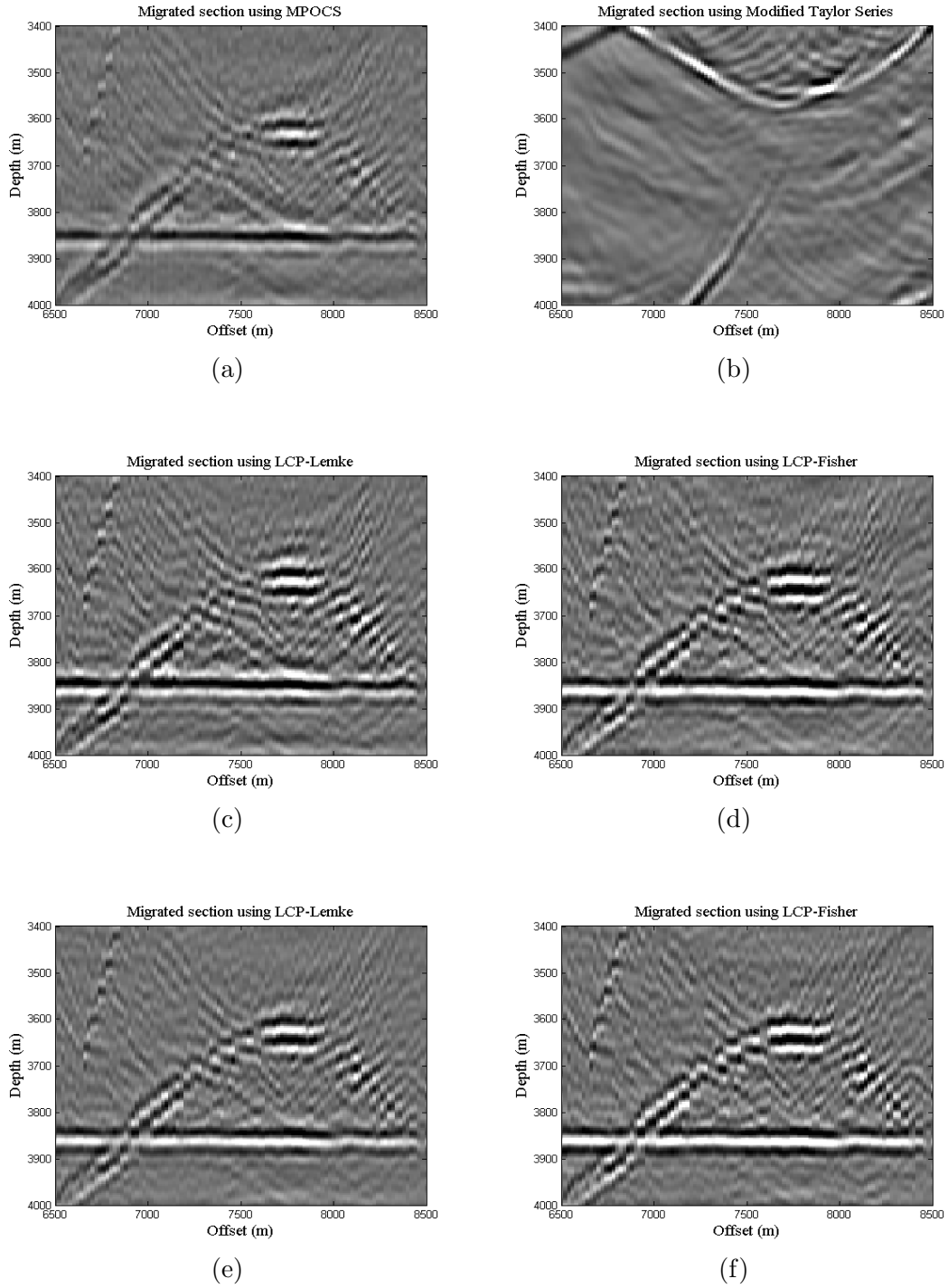


Figure 3.16: Details of a structurally challenging sub-salt area (lateral position of 6500 – 8500m and depth of 3400 – 4000m) using (a) MPOCS [3] ($N = 25$) (b) Modified Taylor Series [2] ($N = 25$)(c) LCP-Lemke ($N = 25$), (d) LCP-Fisher ($N = 25$), (e) LCP-Lemke ($N = 35$), (f) LCP-Fisher ($N = 35$)

3.5 Summary

In this chapter, it was shown that the seismic wavefield extrapolation filter can be formulated as LCP. Performance of two LCP algorithms, Lemke and Fisher-Newton method, was tested. The quality of subsurface images generated by using these filters shows that with 25 coefficients, the LCP Lemke outperforms the LCP Fisher-Newton method while at the same time both LCP algorithms produce better seismic images, when compared to those generated by MPOCS [3] and the modified Taylor series [2]. However, with 35 coefficients both LCP algorithms produce comparable results.

CHAPTER 4

ONE DIMENSIONAL

WAVEFIELD

EXTRAPOLATION FILTER

VIA L_1 ERROR

APPROXIMATION

4.1 Introduction

As described in Chapter 3, 1-D seismic FIR wavefield extrapolation filters designed via linear complementarity problem approach can accommodate higher propagating angles but some of the filters have high error especially at cutoff and it is desirable to produce such filters with small errors to obtain better practically sta-

ble seismic images. Since amplitude distribution given by L_1 norm will tend to have very small residuals, thus, to deal with high passband error, the design problem of 1-D wavefield extrapolation filter is studied via L_1 error approximation. A comparison analysis is shown between both developed methods, LCP and L_1 error approximation. The design of such filters via L_1 norm was proposed in [5] for the purpose of obtaining sparse filter coefficients. In this chapter, the problem will be reformulated to obtain sparse error between the ideal and approximated FIR wavefield extrapolation filter.

4.2 Problem Formulation

Formulation via L_1 error approximation is stated as follows. Again, recall that the 1-D extrapolation filter's wavenumber response can be given by:

$$H(e^{jk_x}) = \sum_{n=0}^M (2 - \delta[n])h[n] \cos(nk_x), \quad (4.1)$$

where $h[n]$ is the impulse response of the 1-D FIR extrapolation filter. After discretizing the K_x to be K_{x_i} , ($i = 1, \dots, L$), (4.1) can be written as following matrix form

$$\mathbf{H}(e^{jk_{x_i}}) = \mathbf{C}\mathbf{h}, \quad i = 1, \dots, L, \quad (4.2)$$

where

$$\mathbf{C} = \begin{bmatrix} 1 & \cos(k_{x_1}) & \cdot & \cdot & \cdot & \cos(Mk_{x_1}) \\ \cdot & \cdot & \cdot & \cdot & \cdot & \cdot \\ \cdot & \cdot & \cdot & \cdot & \cdot & \cdot \\ 1 & \cos(k_{x_k}) & \cdot & \cdot & \cdot & \cos(Mk_{x_k}) \\ \cdot & \cdot & \cdot & \cdot & \cdot & \cdot \\ \cdot & \cdot & \cdot & \cdot & \cdot & \cdot \\ \cdot & \cdot & \cdot & \cdot & \cdot & \cdot \\ 1 & \cos(k_{x_L}) & \cdot & \cdot & \cdot & \cos(Mk_{x_L}) \end{bmatrix}, \quad \mathbf{h} = \begin{bmatrix} h(0) \\ h(1) \\ \cdot \\ \cdot \\ \cdot \\ h(M-1) \\ h(M) \end{bmatrix}. \quad (4.3)$$

The design problem of 1-D FIR wavefield extrapolation filter coefficients is to find \mathbf{h} such that

$$\min_h \|\mathbf{C}\mathbf{h} - \mathbf{H}_d\|_1, \quad (4.4)$$

where $H_d(e^{jk_{x_i}}) = e^{jb\sqrt{K_c^2 - k_{x_i}^2}}$ is the desired wavenumber response. Basically, L_1 error approximation attempts to obtain sparse difference between \mathbf{H}_d (2.2) and $\mathbf{H}(e^{jk_x})$ as given by (4.4). Approximating error via L_1 (4.1) can have few large significant value which are expected to appear at the cutoff. However, in the context of FIR wavefield extrapolation filter, the performance of L_1 norm can be improved by emphasizing more weights on passband wavenumbers, when compared to the stopband as:

$$\min_h \|\mathbf{W}(\mathbf{C}\mathbf{h} - \mathbf{H}_d)\|_1, \quad (4.5)$$

where $\mathbf{W} = \begin{bmatrix} W_p & 0 \\ 0 & W_s \end{bmatrix}$ is the diagonal weighting matrix. If W_p and W_s are passband and stopband weights, respectively, then $W_p \geq W_s$. In the case of FIR extrapolation filter design, $W_p = 10$ and $W_s = 1$. Simulation results will show that L_1 error approximation approach offers advantage to tackle the problem of high passband error of the FIR wavefield extrapolation filter.

4.2.1 Design Algorithm

1. Select the filter length N and cutoff k_c .
2. Formulate matrices \mathbf{H}_d , \mathbf{C} and \mathbf{W} based on equations (2.2), (4.3) and (4.5).
3. Solve the L_1 norm problem in (4.5) to get the filter coefficients.

The proposed, L_1 error approx. based, algorithm for designing the $f - x$ FIR extrapolation digital filters is shown in figure 4.1:

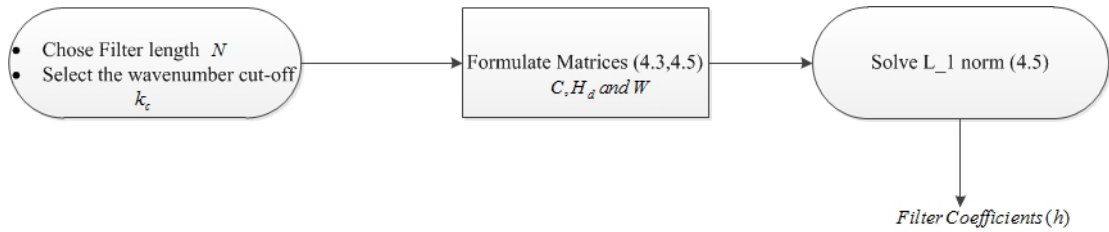


Figure 4.1: L_1 error approximation based work flow of the algorithm to design $f - x$ FIR wavefield extrapolation filters.

4.3 Simulation Results

In this section, a set of design examples is provided of different 1-D FIR wavefield extrapolation filter for decaying parameter $b = 0.2$, a cutoff, $k_c = 0.25$ and various

lengths ($N = 25, 35$). The objective is to show various designs using L_1 error approximation and L_1 norm.

Figure 4.2 and 4.3 show the magnitude and phase performance as well as error in passband of an FIR wavefield extrapolation filter with $N = 25$ and $N = 35$ designed via L_1 error approximation, LCP-Lemke and L_1 norm [5] approaches for cutoff $k_c = 0.25$ and decaying parameter $b = 0.2$.

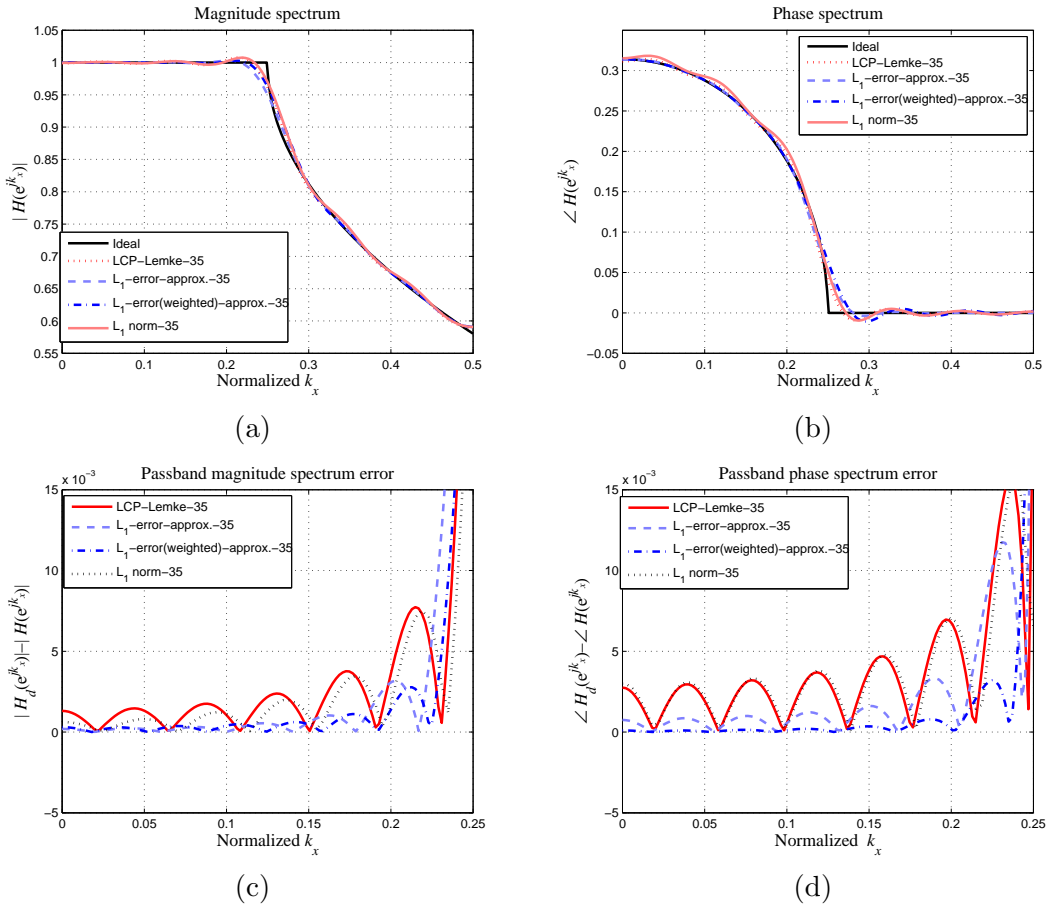


Figure 4.2: (a) Magnitude and (b) phase response of 1-D extrapolation filter designed by L_1 error approximation with and without weights, LCP-Lemke and L_1 norm [5] approach, (c) and (d) show the passband magnitude and phase errors, respectively.

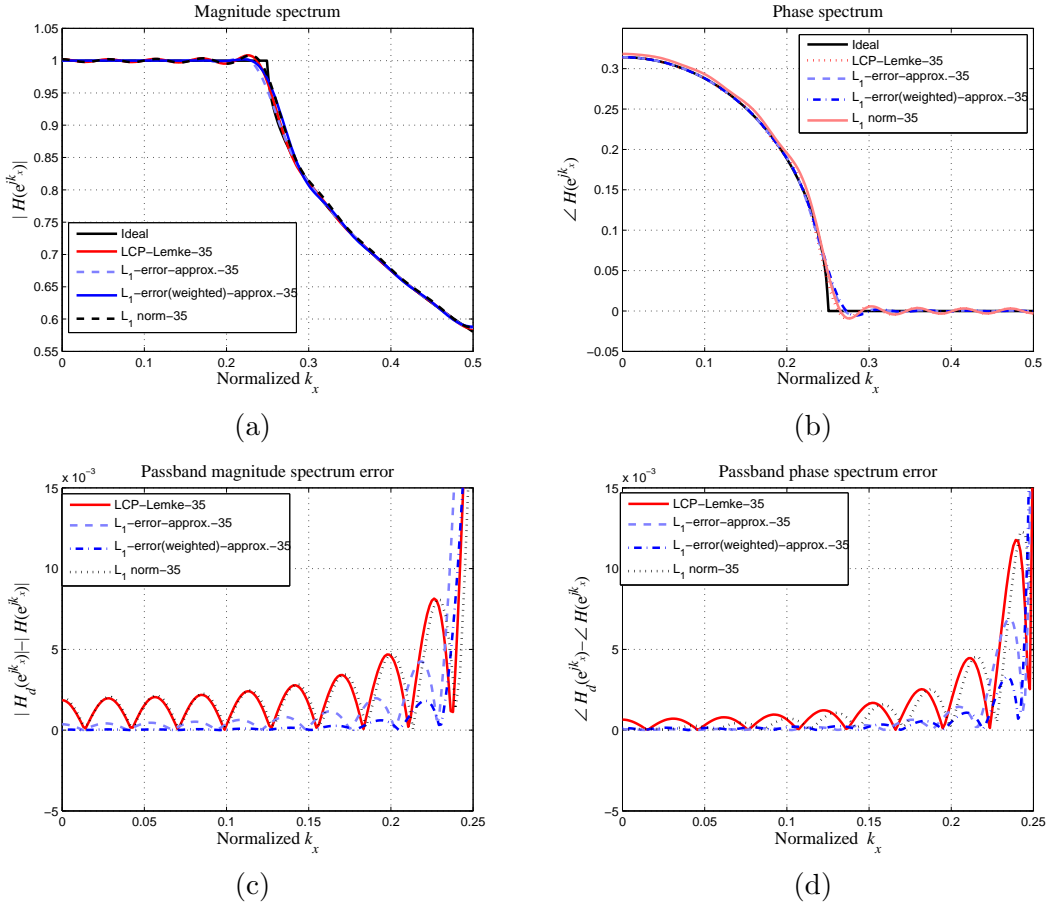


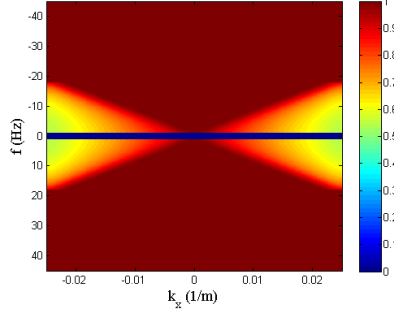
Figure 4.3: (a) Magnitude and (b) phase response of 1-D extrapolation filter designed by L_1 error approximation with and without weights, LCP-Lemke and L_1 norm [5] approach, (c) and (d) show the passband magnitude and phase errors, respectively.

This can be observed that amplitude distribution of the error vector given by L_1 error approximation tend to close to zero. Figure 4.2 and 4.3 show trade off between LCP-Lemke and L_1 error minimization (4.4) and L_1 norm [5], based on passband error and accommodation of higher propagating angles. Since L_1 error approximation method attenuates some of the higher propagating angles, thus this method can effect subsurface image in the heterogeneous media with strong lateral velocity variations. However, in the context of accommodating wider angles, performance of the L_1 error approximation (4.5) becomes better by emphasizing more weights on passband wavenumbers, $W_p \geq W_s$ (4.5). It is clear from the presented examples that weighted L_1 error approximation (4.5) offers solution to the problem of high passband error as well as accommodate the higher propagating angles. On the other hand, it can be seen that LCP-Lemke and L_1 norm [5] accommodates wider propagating angles at the expense of passband error.

4.4 Application to SEG/EAGE Salt Model

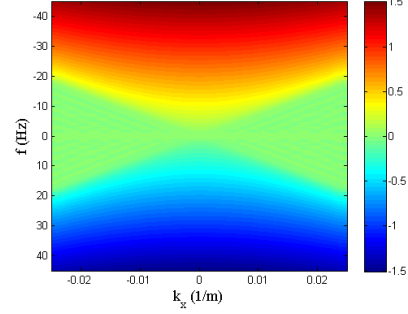
The effectiveness of the proposed L_1 error approximated FIR extrapolation filters has been studied by extrapolating the challenging SEG/EAGE salt velocity model and results are compared with L_1 norm method [5].

Magnitude response of extrapolators designed by L_1 error approx.



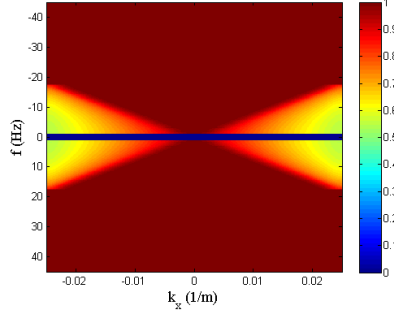
(a)

Phase response of extrapolators designed by L_1 error approx.



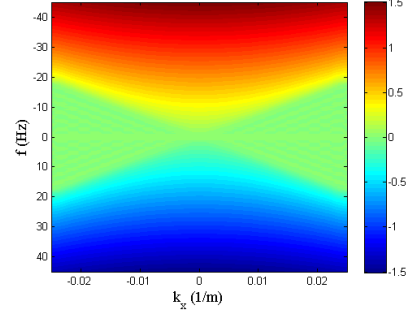
(b)

Magnitude response of extrapolators via weighted L_1 error approx.



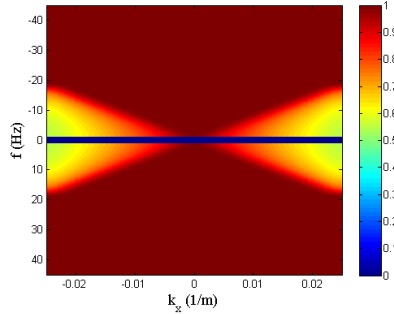
(c)

Phase response of extrapolators via weighted L_1 error approx.



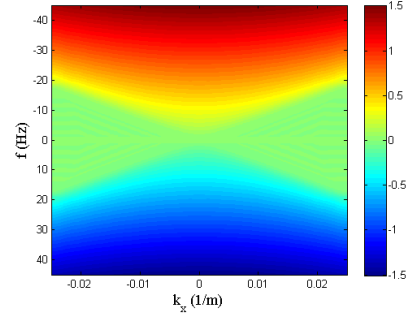
(d)

Magnitude response L_1 norm designed extrapolators



(e)

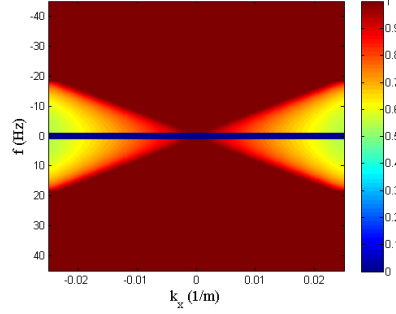
Phase response L_1 norm designed extrapolators



(f)

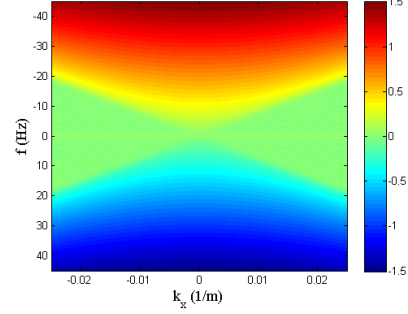
Figure 4.4: Set of designed $f - x$ FIR extrapolation filters in the frequency-wavenumber domain with $N = 25$ (a) and (b) show the magnitude and phase responses of L_1 error approximation (c) and (d) show the magnitude and phase responses of weighted L_1 error approximation and (e) and (f) show the magnitude and phase responses of L_1 norm [5], respectively.

Magnitude response of extrapolators designed by L_1 error approx.



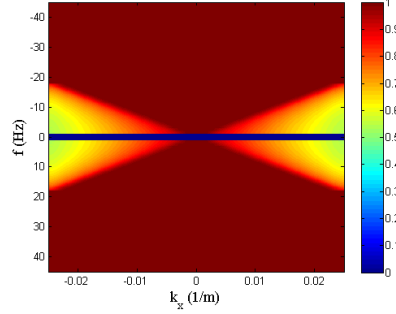
(a)

Phase response of extrapolators designed by L_1 error approx.



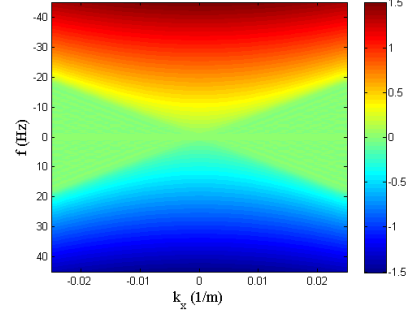
(b)

Magnitude response of extrapolators via weighted L_1 error approx.



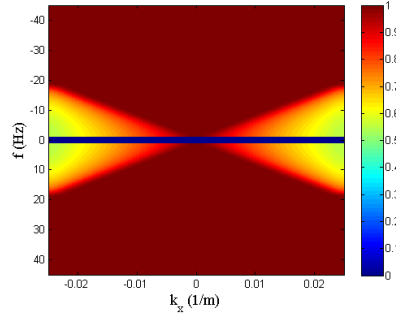
(c)

Phase response of extrapolators via weighted L_1 error approx.



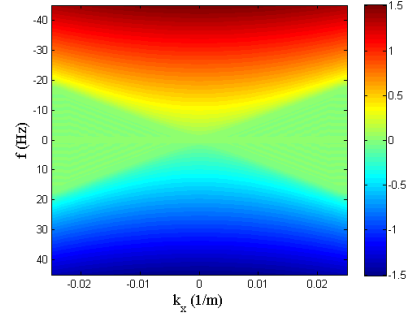
(d)

Magnitude response L_1 norm designed extrapolators



(e)

Phase response L_1 norm designed extrapolators



(f)

Figure 4.5: Set of designed $f - x$ FIR extrapolation filters in the frequency-wavenumber domain with $N = 35$ (a) and (b) show the magnitude and phase responses of L_1 error approximation (c) and (d) show the magnitude and phase responses of weighted L_1 error approximation and (e) and (f) show the magnitude and phase responses of L_1 norm [5], respectively.

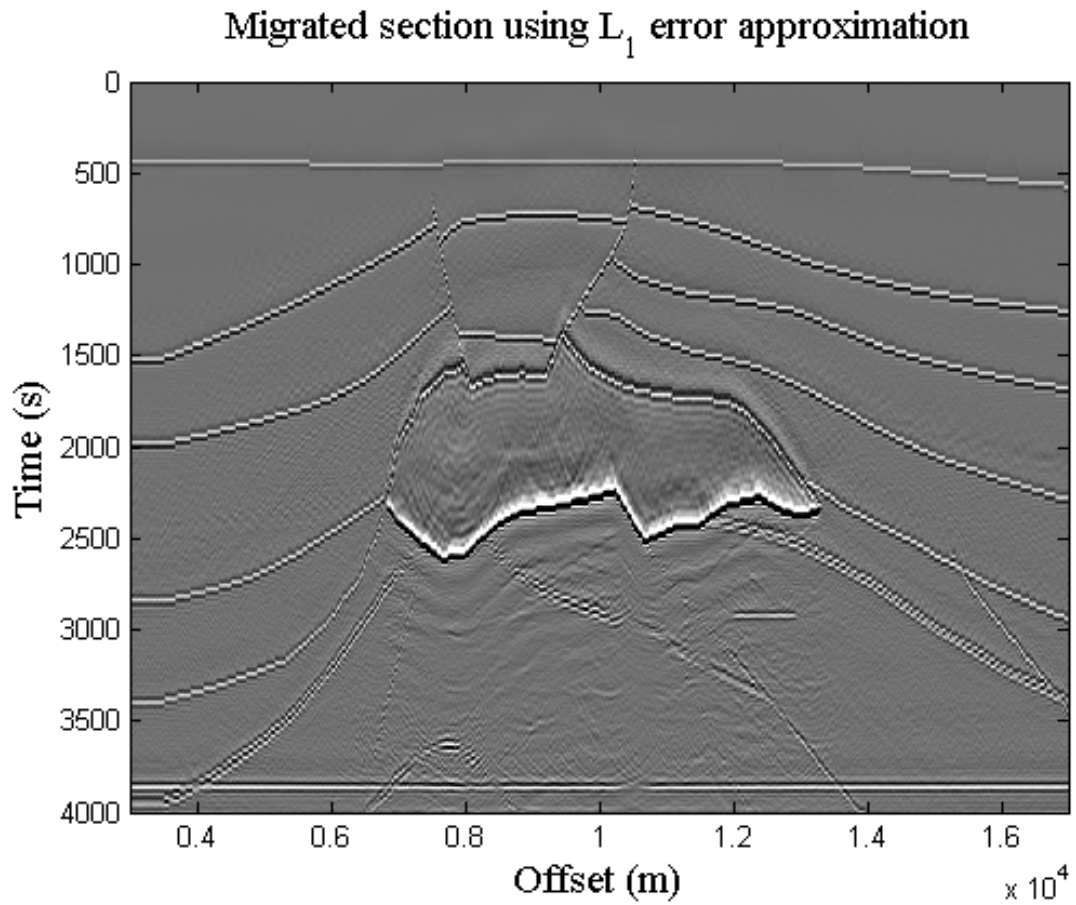


Figure 4.6: Extrapolated SEG/EAGE salt model using L_1 error approximation with 25-coefficients.

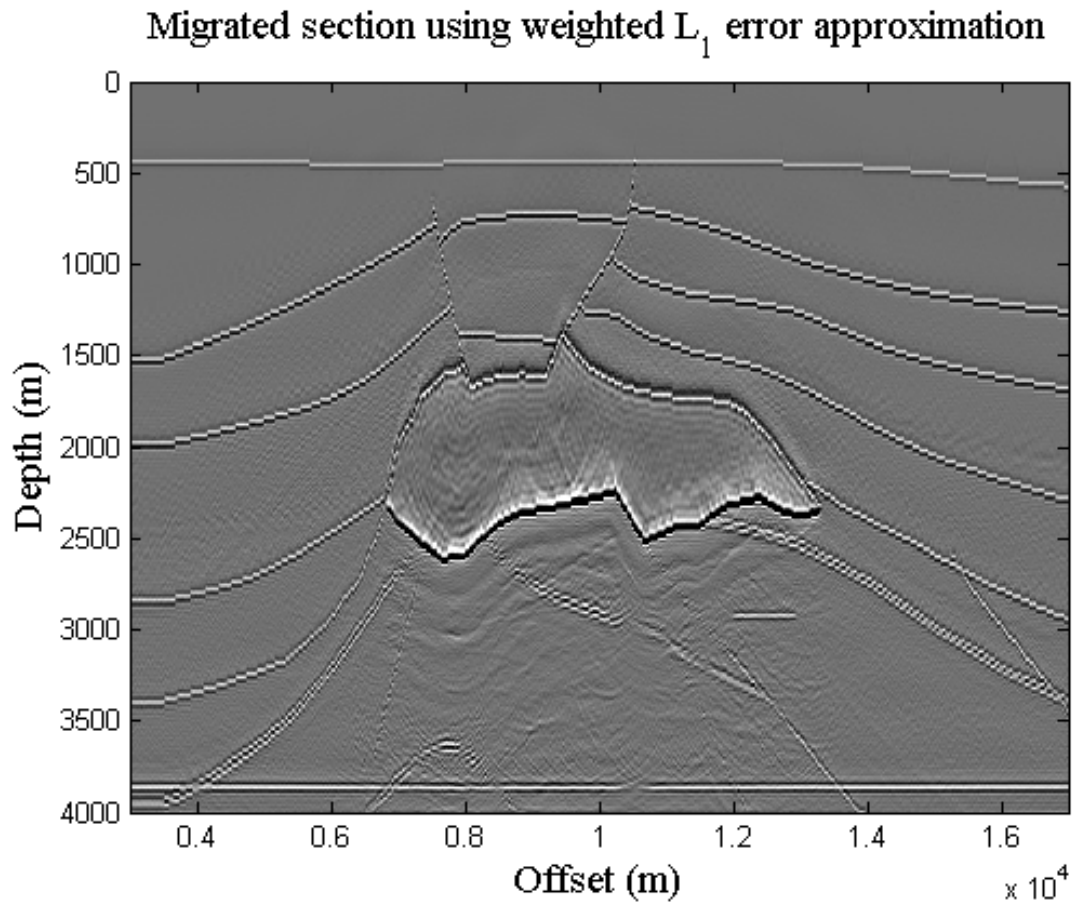


Figure 4.7: Extrapolated SEG/EAGE salt model using weighted L_1 error approximation with 25-coefficients.

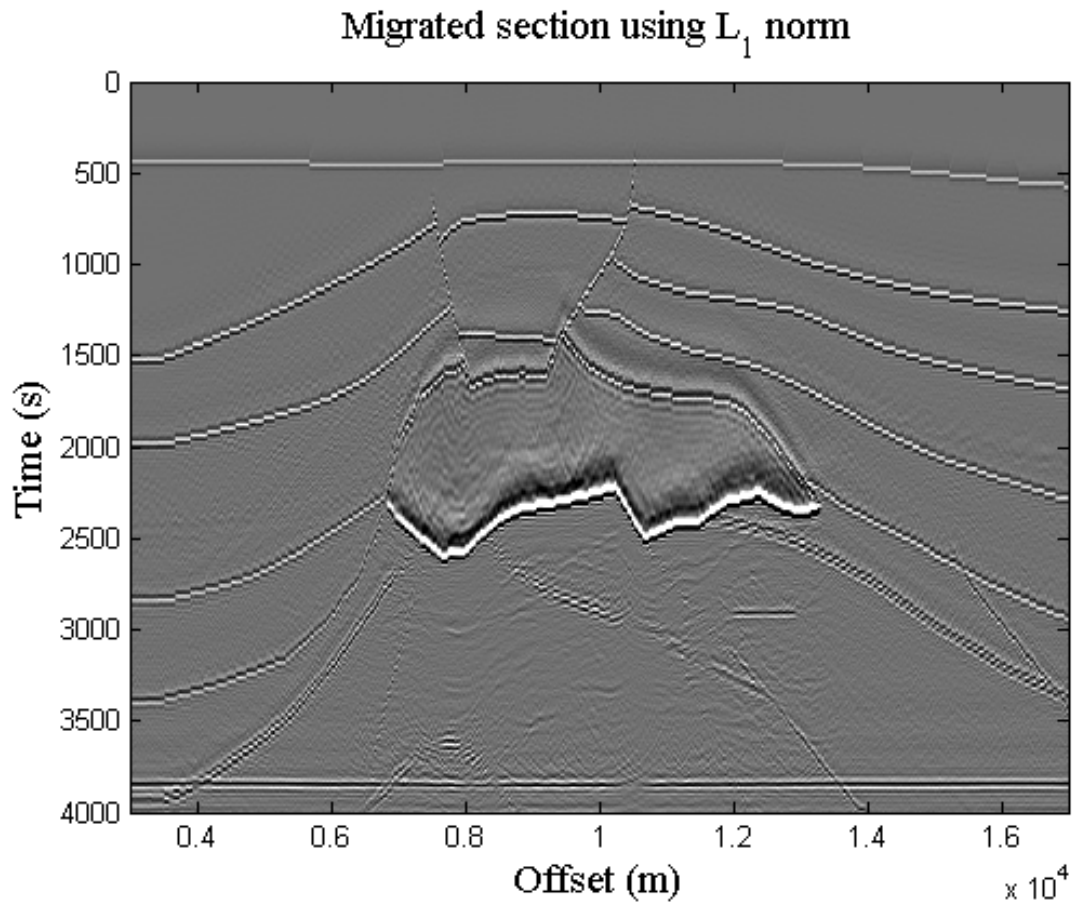


Figure 4.8: Extrapolated SEG/EAGE salt model using L_1 norm [5] with 25-coefficients.

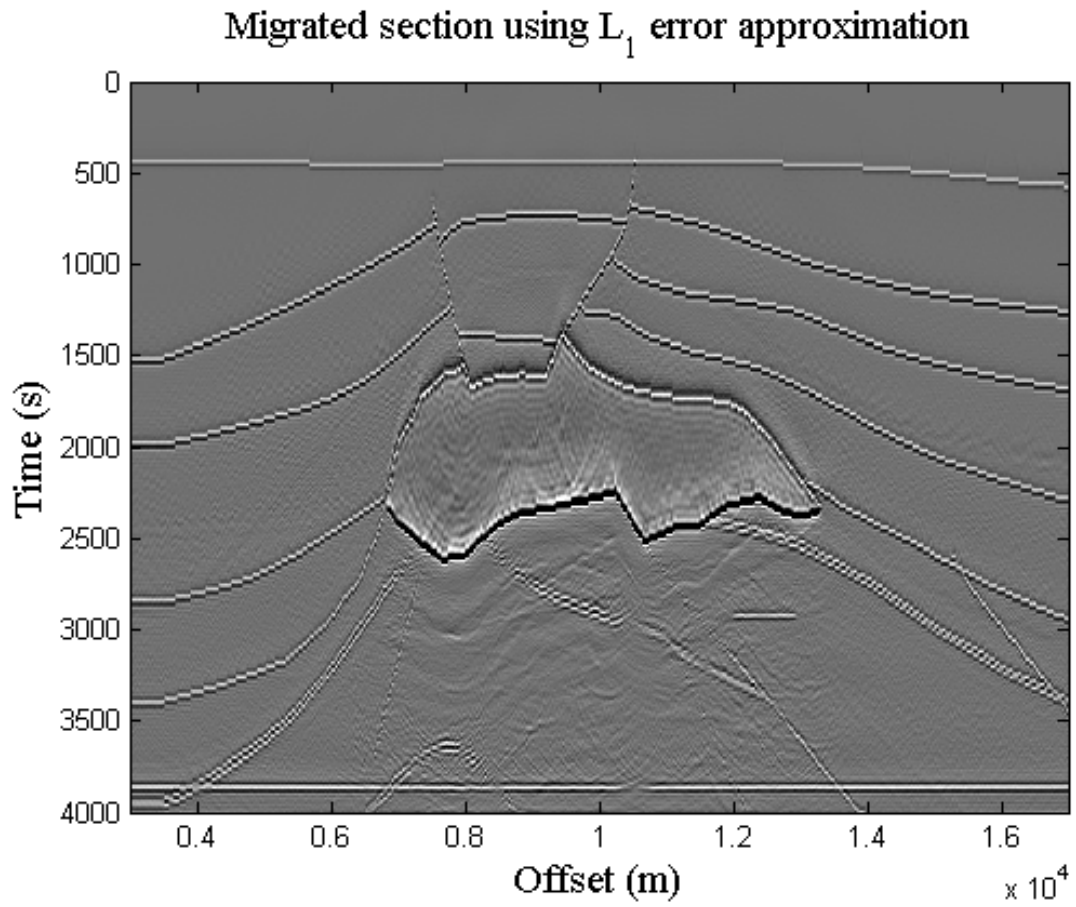


Figure 4.9: Extrapolated SEG/EAGE salt model using L_1 error approximation with 35-coefficients.

Migrated section using weighted L_1 error approximation

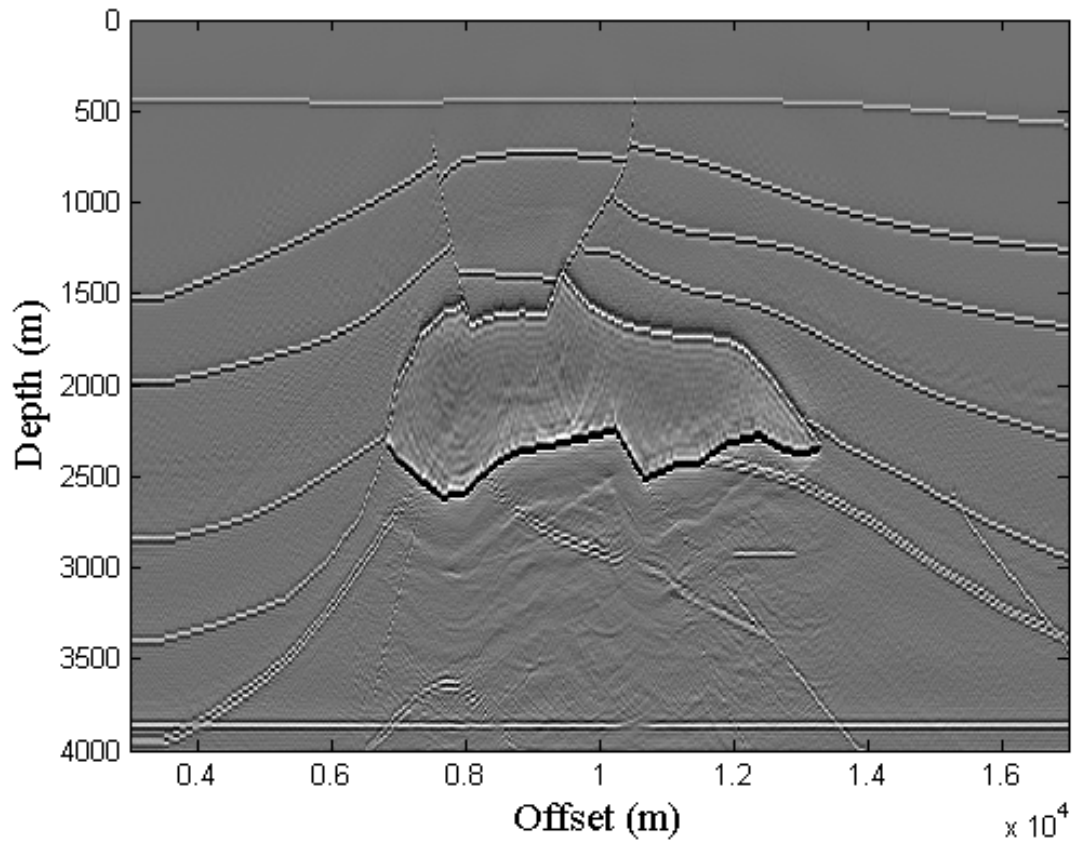


Figure 4.10: Extrapolated SEG/EAGE salt model using weighted L_1 error approximation with 35-coefficients.

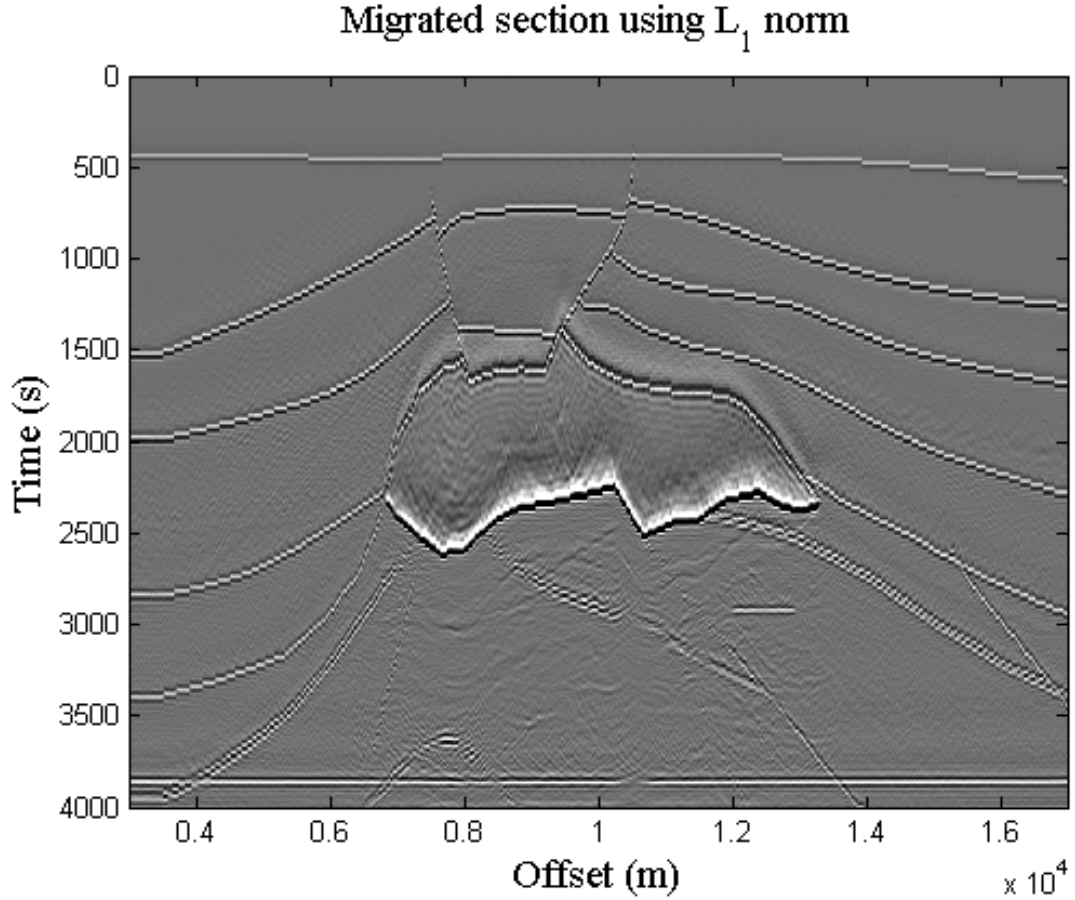


Figure 4.11: Extrapolated SEG/EAGE salt model using L_1 norm [5] with 35-coefficients.

Figures 4.6-4.8 show the subsurface image that has been produced by extrapolated SEG/EAGE salt velocity model using FIR extrapolation filters ($N = 25$) designed by L_1 error approximation, weighted L_1 error approximation and L_1 norm, whereas figure 4.9 -4.11 show the same data extrapolated but with ($N = 35$). These methods lead to stable images but it can be observed that image quality of SEG/EAGE salt model produced by L_1 error approximation is better than L_1 norm [5] method. This is because FIR extrapolation filters designed by L_1 error approximation have the least passband wavenumber response error, when compared to L_1 norm method [5].

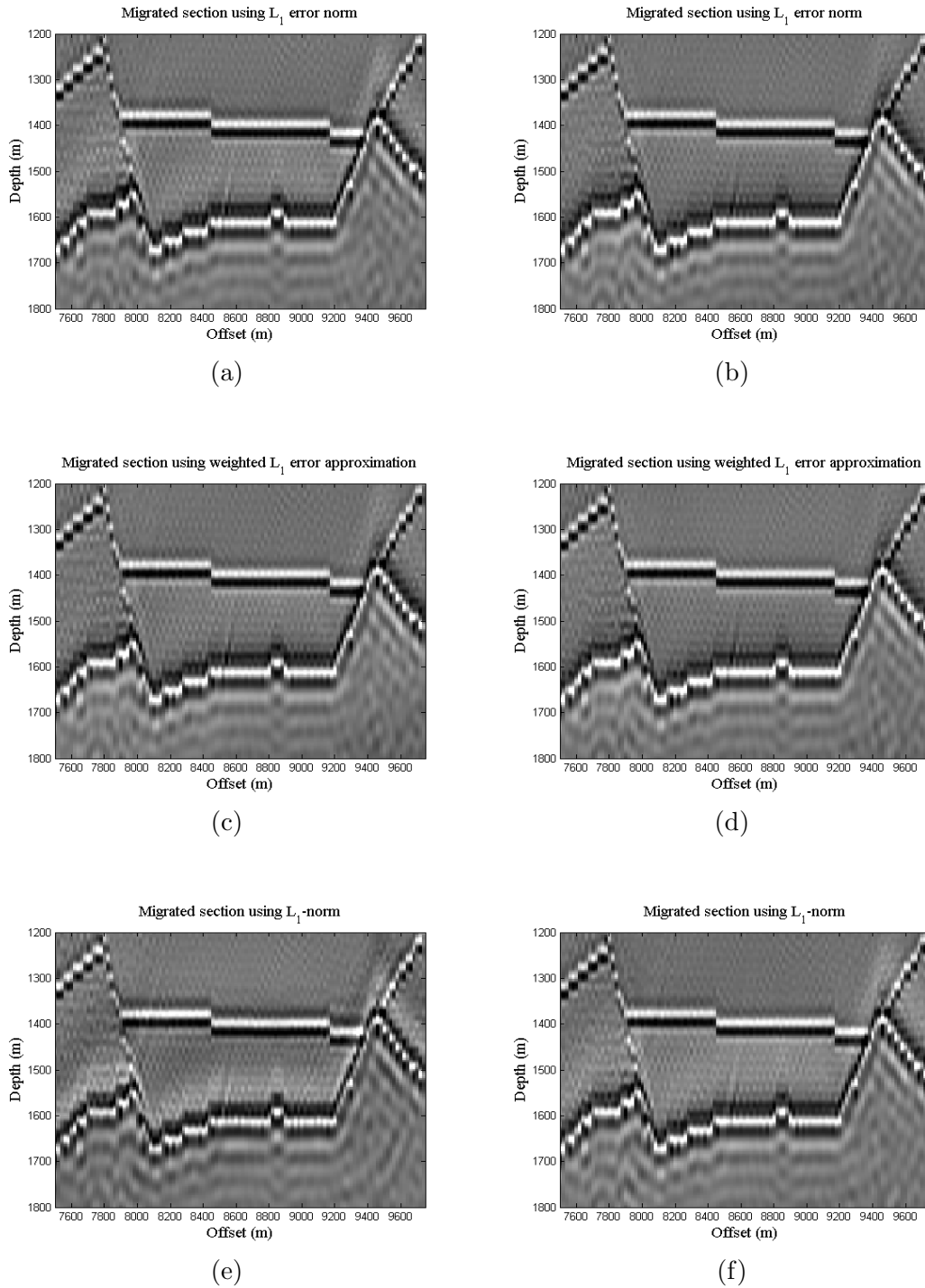


Figure 4.12: Details of an area with different dips (lateral position of 7500–9750m and depth of 1200–1800m) using (a) L_1 error norm ($N = 25$), (b) L_1 error norm ($N = 35$), (c) weighted L_1 error norm ($N = 25$), (d) weighted L_1 error norm ($N = 35$) and (e) L_1 norm [5] ($N = 25$), (f) L_1 norm [5] ($N = 35$)

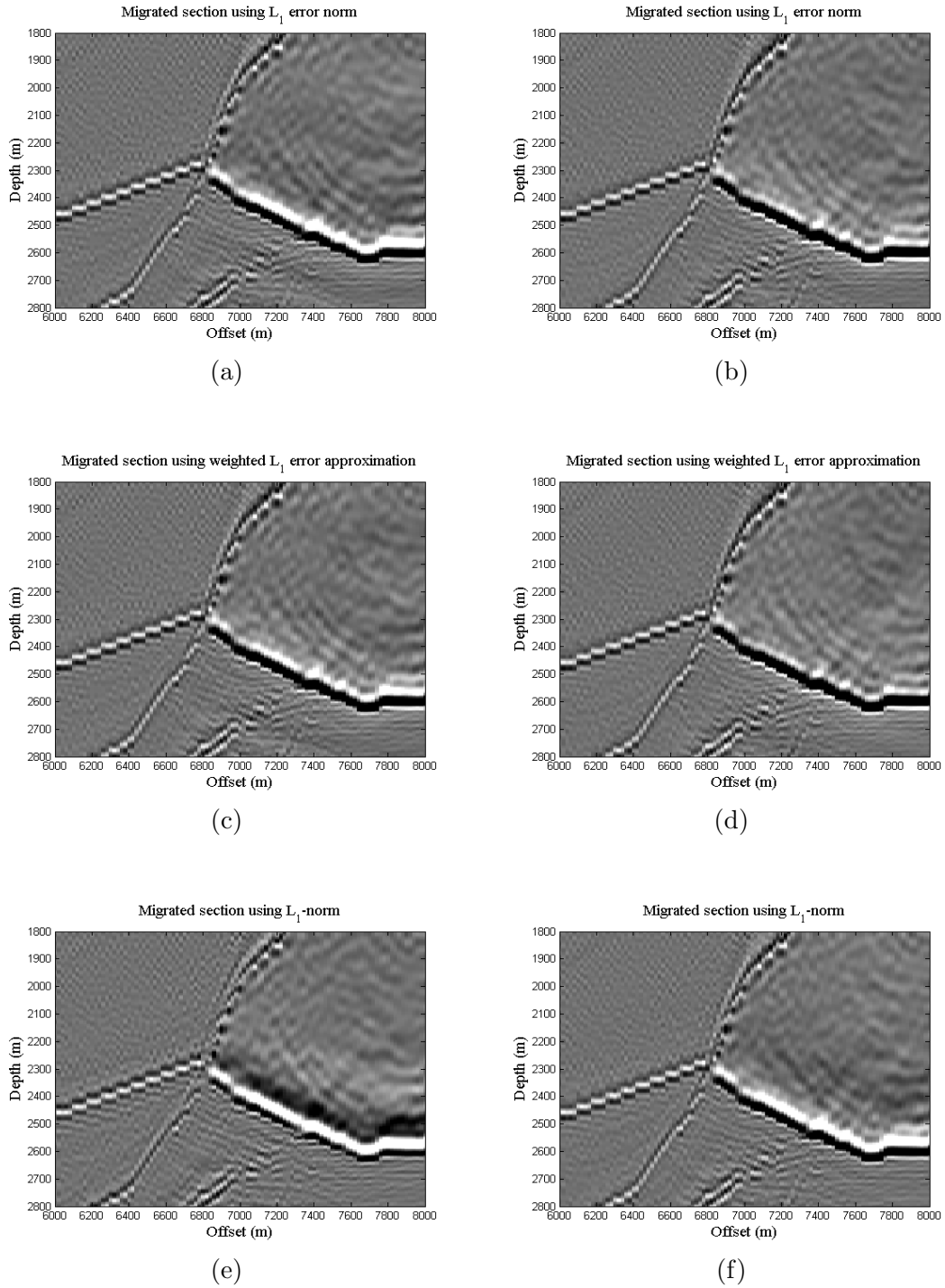


Figure 4.13: Details of an area with steep dips on the left flank of the salt model (lateral position of 6000 – 8000m and depth of 1800 – 2800m) using (a) L_1 error norm ($N = 25$), (b) L_1 error norm ($N = 35$), (c) weighted L_1 error norm ($N = 25$), (d) weighted L_1 error norm ($N = 35$) and (e) L_1 norm [5] ($N = 25$), (f) L_1 norm [5] ($N = 35$)

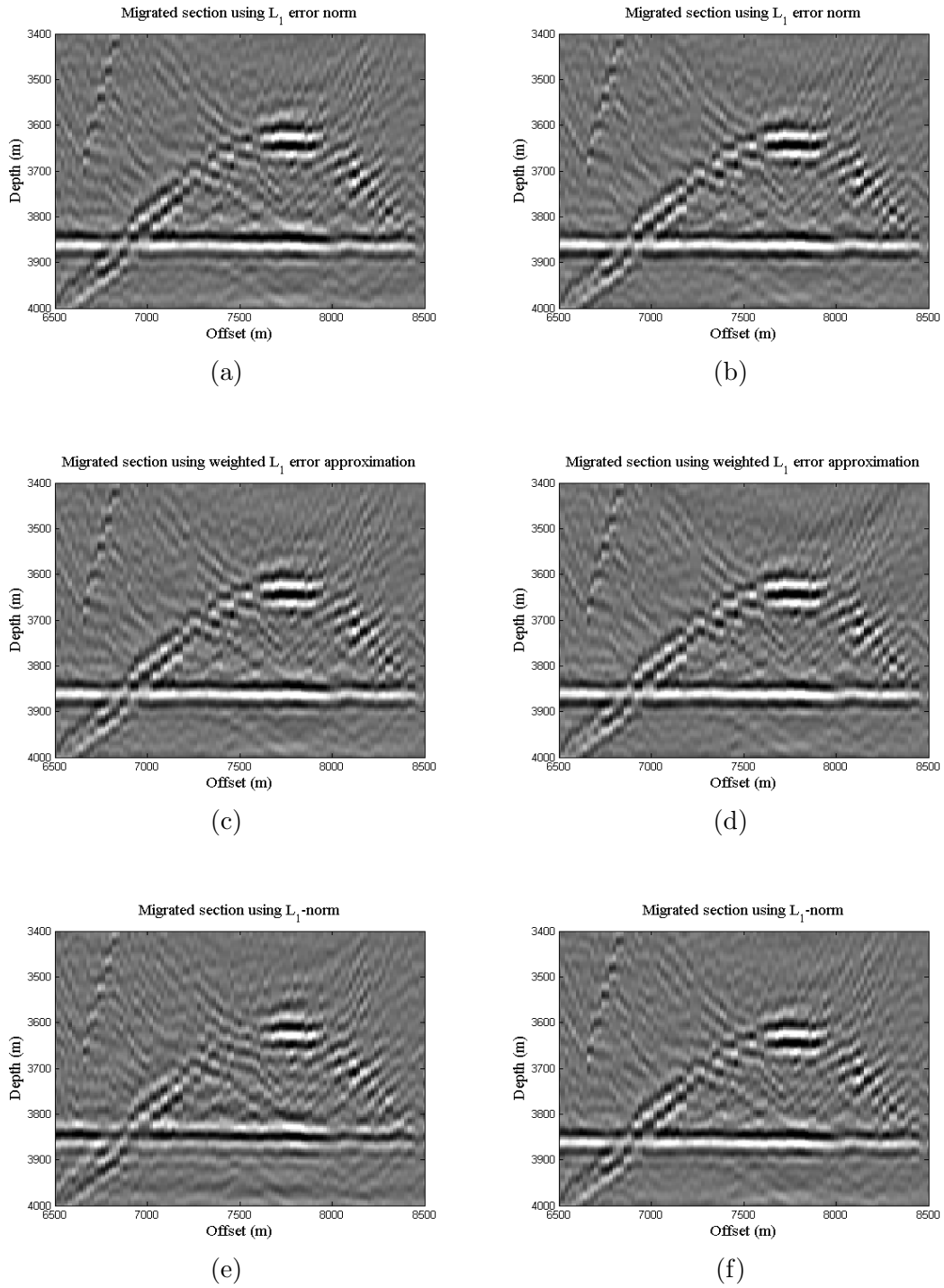


Figure 4.14: Details of a structurally challenging sub-salt area (lateral position of 6500 – 8500m and depth of 3400 – 4000m) using (a) L_1 error norm ($N = 25$), (b) L_1 error norm ($N = 35$), (c) weighted L_1 error norm ($N = 25$), (d) weighted L_1 error norm ($N = 35$) and (d) L_1 norm [5] ($N = 25$), (e) L_1 norm [5] ($N = 35$).

4.5 Summary

As described in chapter 2, small wavenumber errors are one of the design requirement for FIR extrapolation filters. Since L_1 norm is known to give a solution with values close to zero. In this chapter, above property of L_1 norm has been exploited by formulating the design problem of 1-D FIR extrapolation filter via L_1 error approximation. The Performance comparison of the L_1 error approximation method with LCP and L_1 norm [5] shows that it offer small passband error at the cost of attenuating some of the higher propagating angles. However, L_1 error approximation not only offers small error in the passband but also accommodate wider propagating angles by emphasizing more weights on passband wavenumbers $W_p \geq W_s$ (4.5). It is interesting to note that in [5], author applied L_1 norm on the solution vector to get sparse solution while here, L_1 norm is enforced on the error vector to get insignificant error values, i.e., values close to zero.

CHAPTER 5

CONCLUSION AND FUTURE WORK

In this research work, the problem of complex-valued Finite Impulse Response(FIR) wavefield extrapolation filter design is considered as a linear complementarity problem (LCP). LCP is not an optimization technique as there is no objective function to optimize, however, quadratic programming, one of the applications of LCP, can be used to find optimal solution for 1-D FIR wavefield extrapolation filter. The design problem is formulated via quadratic programming and then equivalent semi-definite LCP form is obtained by applying the Kuhn Tucker conditions. There are basically two families to solve semi-definite LCP: *a)* direct algorithms *b)* indirect algorithms. Lemke (direct) and Fisher-Newton method (indirect) have been tested for the resulted LCP. Being direct, Lemke's algorithm is the most robust and computationally efficient when compared to Fisher-Newton method. Both result in stable seismic images. This was

shown for SEG/EAGE salt velocity model, however some of the designed extrapolators needed to be stabilized. At the same time, the LCP-Lemke was producing more stable images, while the LCP-Fisher was producing ghost events on the SEG/EAGE salt images.

To deal with laterally varying velocity, one of the challenge in designing FIR wavefield extrapolator is to keep passband error as small as possible with smallest possible filter length. To deal with passband error, L_1 error approximation approach is introduced. The idea is to find sparse error between the ideal and approximated FIR extrapolator. Presented examples in chapter 4 show that with weighted L_1 error approximation approach produce small magnitude and phase error as well as accommodate wavefields propagating with high angles. The seismic images of the 2-D SEG/EAGE model were, therefore, stable and better with those obtained via L_1 norm [5].

5.1 Future Work

Following are the important suggestions to further extending the developed theories of LCP and L_1 error approximation in the context of seismic wavefield extrapolation.

5.1.1 Efficient LCP Solvers

It has been shown that the design of 1-D FIR wavefield extrapolation filters is an example of a semi-definite LCP. There exist many algorithms to solve semi-definite LCP including Lemke's algorithm. In the FIR wavefield extrapolation filter case, one has to solve for the filter coefficient but also for slack variables. It is suggested to make a modification in Lemke algorithm such that it terminates after finding filter coefficients.

The disadvantage of LCP is that it can not exploit the matrix properties in the case of 2-D filters. Modifications should be made in LCP structure so that it can be applied to design 2-D filters.

5.1.2 Optimal tradeoff between different norms

Holdberg [27] looked into the problem of seismic wavefield extrapolation filter via the L_2 norm. Though the designed extrapolation filters cover wider angles, they introduce high errors especially at the cutoff. Hence, this method can only be used for smaller depths. While on the other hand, designed extrapolation filters via L_1 error approximation without weights (4.4) offer less passband error, so the extrapolation filters designed via this method can extrapolate wavefield for larger depths but on the cost of attenuating the higher propagating angles. Depending upon different requirements, one can find optimal trade off between L_2 and L_1

error approximation that sacrifices a slightly higher error to include wider angles.

APPENDIX A

LINEAR COMPLIMENTARITY PROBLEM

The latter details are gathered from [38, 39, 53] to provide better understanding about the mathematical structure of LCP as well as its solver, Lemke the path following algorithm, and Kuhn Tucker conditions.

A.1 Mathematical Structure of LCP

The Linear Complimentarity Problem deals with finding a vector in finite dimensional real vector space that satisfies certain inequalities. Specifically, given a vector $q \in R^n$ and a Matrix $M \in R^{n \times n}$, the linear complimentarity problem finds

a vector $z \in R^n$ such that [39]:

$$\left. \begin{aligned} z &\geq 0 \\ q + Mz &\geq 0 \\ z^T(q + Mz) &= 0 \end{aligned} \right\}, \quad (\text{A.1})$$

or shows that no such vector z exists. The linear complementarity problem, abbreviated as LCP, sometimes denoted by the pair (q, M) .

A.2 Source Problems

The Linear Complementarity Problem is not an optimization technique but it unifies the linear, quadratic programs as well as bi-matrix game problems. Quadratic programs are extremely important source of application for the LCP. There are several highly effective algorithms for solving Quadratic programs that are based on the LCP. A significant number of applications in engineering and physical sciences including the journal bearing problem, the elastic-plastic torsion problem and filter design problem etc lead to convex quadratic programming which is equivalent to the linear complementarity Problem.

A.2.1 Application to Quadratic Programming

A quadratic program is an mathematical optimization problem having a quadratic objective function subject to linear constraints. A significant number of applications in engineering including filter design problem lead to convex quadratic

programming which is extremely important source of application of the linear complementarity problem. A quadratic program can be written as [38, 39]

$$\begin{aligned} & \text{Minimize } c^T x + \frac{1}{2} x^T Q x \\ & \text{Subject to } Ax \leq o \\ & x \geq 0, \end{aligned} \tag{A.2}$$

where

$$c \in R^n, \quad \text{symmetric matrix } Q \in R^{n \times n}, \quad A \in R^{m \times n}, \quad b \in R^m.$$

The case $Q = 0$ give rise to a linear program. If objective function is convex then Q is semidefinite positive and the sufficient Kuhn-Tucker conditions for global optimal solution of the quadratic program are that there must exist vectors $u \in R^n, v \in R^m,$ and $\lambda \in R^m$ such that [38, 39]:

$$\begin{aligned} c + Qx + A^T \lambda - u &= 0 \\ Ax + v &= b \\ u \geq 0, v \geq 0, x \geq 0, \lambda \geq 0, u^T x &= 0, v^T \lambda = 0, \end{aligned} \tag{A.3}$$

clearly, this can be written as

$$\begin{aligned} \begin{pmatrix} u \\ v \end{pmatrix} &\equiv \begin{pmatrix} c \\ b \end{pmatrix} + \begin{pmatrix} Q & A^T \\ -A & 0 \end{pmatrix} \begin{pmatrix} x \\ \lambda \end{pmatrix} \\ u \geq 0, v \geq 0, x \geq 0, \lambda \geq 0, u^T x &= 0, v^T \lambda = 0. \end{aligned} \tag{A.4}$$

Quadratic program is therefore an example of the linear complementarity problem

(q, M) where

$$q = \begin{pmatrix} c \\ b \end{pmatrix}, \quad \text{and} \quad M = \begin{pmatrix} Q & A^T \\ -A & 0 \end{pmatrix}.$$

Example:

$$\text{Minimize } -8x_1 - 16x_2 + x_1^2 + 4x_2^2$$

$$\text{Subject to } x_1 + x_2 \leq 5$$

$$x_1 \leq 3$$

$$x_1 \geq 0$$

$$x_2 \geq 0,$$

The above program can be written as:

$$\text{Minimize } c^T x + \frac{1}{2} x^T Q x$$

$$\text{Subject to } Ax \leq 0$$

$$x \geq 0,$$

where

$$c = \begin{pmatrix} -8 \\ -16 \end{pmatrix}, \quad Q = \begin{pmatrix} 2 & 0 \\ 0 & 8 \end{pmatrix}, \quad A = \begin{pmatrix} 1 & 1 \\ 1 & 0 \end{pmatrix}, \quad b = \begin{pmatrix} 5 \\ 3 \end{pmatrix}.$$

The LCP form of the given quadratic program is as follows

$$M = \begin{pmatrix} Q & A^\tau \\ -A & 0 \end{pmatrix} = \begin{pmatrix} 2 & 0 & 1 & 1 \\ 0 & 8 & 1 & 0 \\ -1 & -1 & 0 & 0 \\ -1 & 0 & 0 & 0 \end{pmatrix}, \quad q = \begin{pmatrix} c \\ b \end{pmatrix} = \begin{pmatrix} -8 \\ -16 \\ 5 \\ 3 \end{pmatrix}.$$

An direct Lemke 's algorithm has been applied to solve (q, M) , which produces following results

$$x = \begin{pmatrix} 3 \\ 2 \end{pmatrix} \quad \text{Minimum value} = -31$$

A.3 Algorithms

Mathematicians over the period of time have developed many direct and indirect methods [39,43] to solve semi-definite LCP. In pivoting (direct) methods, Lemke's algorithm is the most robust algorithm. In 1968 Lemke proved that if M is semi-definite positive, then Lemke's algorithm finds an linear complimentarity solution or shows that no solution exists.

A.3.1 Homotopy Approach

Lemke algorithm can be explained in different ways [38, 39, 53] and homotopy approach is one of these. In path following that is homotopy approach, we start with another system to which we already know the answer. Usually, this is a particular system that has an obvious solution. We then take this simple system

and mathematically bend it into the original system. While bending the system we carefully watch the solution, as it also bends from the obvious solution into the solution we seek. This bending notion underlies a key idea of the homotopy concept.

The homotopy system for LCP:

Given q and M , first choose a positive vector $d \in R^n$ such that $d + q > 0$.

Then consider the following linear complementarity

$$\begin{aligned} z &= d + q + Mx \\ z &\geq 0, \quad x \geq 0, \quad z^T x = 0, \end{aligned} \tag{A.5}$$

clearly, (A.5) has a trivial solution $x = 0$ where $z = d + q$.

Now define homotopy

$$H_t = \min \{x_i, z_i\} = 0, \quad i = 1, \dots, n \tag{A.6}$$

for $z \equiv (1 - t)d + q + Mx$, we see that (A.6) is precisely equivalent to the LC problem

$$z^T x = 0, \quad x \geq 0, \quad z \geq 0$$

where

$$z \equiv (1 - t)d + q + Mx \tag{A.7}$$

At $t = 0$, notice that the trivial LC (A.5) with trivial solution $x = 0$ is obtained, whereas when $t = 1$, we have the original LC (A.1).

(A.7) provides the homotopy system for our procedure. Lemke's algorithm operates on it and generates a path starting from $(x, t) = (0, 0)$. The path will either diverge to infinity or reach $t = 1$. If path reaches $t = 1$, then the lemke algorithm obtains a solution to the LC (A.1)

A.3.2 Lemke the path following Algorithm

Lemke's method traces the path starting from $(x, t) = (0, 0)$ of the homotopy

$$H_t = \min \{x_i, z_i\} = 0, \quad i = 1, \dots, n \quad (\text{A.8})$$

where

$$z \equiv (1 - t)d + q + Mx \quad (\text{A.9})$$

To avoid degeneracies a regularity condition is required:

For each (x, t) in the path, at least $n - 1$ of the variables x, z are greater than zero.

The above condition will be much more clear at the end of this section. To develop Lemke's algorithm, the system (A.9) can be restated as

$$\begin{aligned} Iz - Mx + td &= d + q \\ x \geq 0, \quad z &\geq 0 \\ z^T x &= 0 \end{aligned} \quad (\text{A.10})$$

where I is the identity matrix. This system will turn out to be very convenient, and to understand it let us first analyze the requirement that for i , $z_i x_i = 0$.

To build understanding about Lemke's algorithm, it is necessary to understand the concept of zero set.

Zero set:

we call term x_i the complement of z_i , and vice versa. Clearly, there are n pairs of complementary variables, and by (A.8) either $x_i = 0$ or $z_i = 0$ or possibly both. This is, at least one of the two complementary variables $x_i = 0$ or $z_i = 0$ must be equal to zero, and this holds for all n pairs.

At any step Lemke's algorithm for each i designates either $x_i = 0$ or $z_i = 0$ to be zero throughout that step. Explicitly, there is a zeros set at step k

$$B^k = \{u_1, u_2, u_3, \dots, u_n\}$$

where u_i is a set to either $x_i = 0$ or $z_i = 0$. Throughout the entire step k Lemke's algorithm requires that all $u_i = 0$. To reiterate, on step k , u_i is set equal to x_i or z_i and $u_i = 0$ throughout that step.

The zero set is the key to Lemke's algorithm. To understand it, call w_i the complement of u_i . If $u_i \equiv x_i$, then $w_i \equiv z_i$, and conversely. Because u_i is in the zero set, it must be zero throughout the step, however, the w_i can be zero or positive.

In particular, given B^k , notice (A.10) can be expressed as the $n \times (n + 1)$ system

$$A^k w + t d = d + q \tag{A.11}$$

$$w \geq 0, t \in R^1$$

where for $i = 1, \dots, n$ if

$$u_i \equiv x_i = 0$$

then

$$w_i \equiv z_i, \quad A_i^k \equiv e^i$$

and if

$$w_i \equiv z_i = 0$$

then

$$w_i \equiv x_i, \quad A_i^k \equiv -M_i$$

Here A_i^k is the i th column of A^k . The column e^i (a 1 in the i th position and zeros elsewhere) is associated with $w_i \equiv z_i$ and $-M_i$ is associated with $w_i \equiv x_i$.

The procedure to execute one step of Lemke's algorithm is presented next.

Step k :

On step k we are at a point (x^k, t^k) and the zero set B^k is given. Also, a distinguished variable w_l is specified such that $w_l = 0$. Thus at (x^k, t^k) the variables $u_i = 0, i = 1, \dots, n$, because these variables are in the zero set and also $w_l = 0$.

From B^k we obtain the corresponding (A.11). More ever, at (x^k, t^k) there are

already $n + 1$ variables at zero, so by regularity condition

$$w_i > 0, \quad i \neq l$$

This means that distinguished variable w_l can be increased in (A.11) by adjusting the other $w_i, i \neq l$ and t .

Now in (A.11) increase w_l and suppose that for some positive w_l a variable w_j becomes zero. The point where that occurs is (x^{k+1}, t^{k+1}) and we start the next step, $k + 1$. Thus increase w_l in (A.11) until some variable w_j hits zero, and that starts the next step, $k + 1$.

For step $k + 1$ the new zero set B^{k+1} is formed as follows. The variable w_j that just hits to zero goes into the zero set and its complement u_j comes out. All other variables that were in B^k remain in B^{k+1} . Thus B^{k+1} is the same as B^k except the variable that hit zero goes in and its complement comes out. More over, the complement of w_j becomes the new distinguished variable that is to be increased. In brief, the variable that hits zero enters the zero set. Its complement both comes out and is the new distinguished variable to be increased.

From the new B^{k+1} we can form the corresponding (A.11). Then increase the new distinguished variable just as before. The process continues in this manner.

Summary of Lemke's algorithm:

Step 0

Initially, $(x^0, t^0) = (0, 0)$, $B^0 = \{x_1, \dots, x_n\}$. Increase t from zero in the system

$$z + td = d + q \tag{A.12}$$

$$z \geq 0, \quad t \in R^1$$

- If t can be increased to 1, the $x = 0, z = q \geq 0$, is an LC solution.
- Otherwise, some z_i becomes zero in (A.12) for $t = t^1$. Let $(x^1, t^1) = (0, t^1)$, $w_l = x_i$ be the distinguished variable and

$$B^1 = \{x_1, \dots, x_{l-1}, z_l, x_{l+1}, \dots, x_n\}$$

Go to step 1.

Step k, k ≥ 0

Let (x^k, t^k) be the current point, w_l the distinguished variable and $B^k = u_1, \dots, u_n$ the zero set. Set $u_1 = \dots = u_n = 0$. Then (A.12) becomes

$$A^k w + td = d + q \tag{A.13}$$

$$w \geq 0, \quad t \in R^1$$

where A^k and w are defined by (A.11). Increase w_l from zero in (A.13).

- If t becomes equal to 1, terminate. We have an LC solution at hand.

- If w_l increase to infinity in (A.13), terminate. We have path diverging to infinity.
- otherwise, some w_j becomes zero in (A.13) when $w_l = \bar{w}_l$

Let (x^{k+1}, t^{k+1}) be the new point corresponding to $w_l = \bar{w}_l$, the complement of w_l be the distinguished variable, and $B^{k+1} = u_1, \dots, u_{j-1}, w_j, u_{l+1}, \dots, u_n$.

Go to step $k + 1$.

Repeat this process until $t = 1$ or the path diverges to infinity. *Observe that as w_l increased from (x^k, t^k) , only one variable can hit zero. By regularity condition, at least $n - 1$ variables must be positive. All n variables in the zero set remain zero, so $u_i = 0, i = 1, \dots, n$. If two or more w_j hit zero at once, there would be $n - 2$ or fewer variables positive. Consequently, as we increase w_l , only one variable can hit zero.*

Example:

Let

$$q = \begin{pmatrix} -2 \\ -1 \end{pmatrix} \quad M = \begin{pmatrix} 2 & 1 \\ -1 & 3 \end{pmatrix} \quad d = \begin{pmatrix} 3 \\ 2 \end{pmatrix}$$

Then the system $z = (1 - t)d + q + Mx$ is

$$z_1 - 2x_1 - x_2 + 3t = 1$$

$$z_2 - x_1 - 3x_2 + 2t = 1$$

Step 0. $(x^0, t^0) = (0, 0, 0)$. $B^0 = \{x_1, x_2\}$. The system $A^0 w + td = d + q$ is

$$z_1 = 1 - 3t$$

$$z_2 = 1 - 2t$$

we increase t to $t^1 = \frac{1}{3}$. Then $(x^1, t^1) = (0, 0, \frac{1}{3})$, the distinguished variable variable is x_1 and $B^1 = \{z_1, x_2\}$.

Step 1. The system $A^1 w + td = d + q$ is

$$-2x_1 + 3t = 1$$

$$z_2 + x_1 + 2t = 1$$

we increase x_1 to $x_1^2 = \frac{1}{7}$. Then $(x^2, t^2) = (\frac{1}{7}, 0, \frac{3}{7})$, the distinguished variable variable is x_2 and $B^2 = \{z_1, z_2\}$.

Step 2. The system $A^2 w + td = d + q$ is

$$t = x_2 + \frac{3}{7}$$

$$x_1 = \frac{1}{7} + x_2$$

Increase x_2 to $x_2^3 = \frac{4}{7}$, so that $(x^3, t^3) = (\frac{5}{7}, \frac{4}{7}, 1)$. The point $(\frac{5}{7}, \frac{4}{7})$ is an LC solution.

For more in-depth knowledge of linear complementarity problem and its solution please see [38, 39]

APPENDIX B

CONVEXITY AND K-T CONDITIONS

B.1 Convex Set

convexity is the fundamental concept in the theory of optimization.

consider any two points $x^1, x^2 \in R^n$. The line segment between them is described by the point

$$w = \theta x^1 + (1 - \theta)x^2 \tag{B.1}$$

As θ varies between 0 and 1. Convex sets have the property that the line segment connecting any two points in the set. Mathematically, a set $C \subset R^n$ is convex if

$$x^1, x^2 \in C \tag{B.2}$$

implies that

$$w = \theta x^1 + (1 - \theta)x^2 \in C \text{ for any } \theta, 0 \leq \theta \leq 1 \quad (\text{B.3})$$

Some familiar properties of convex sets are as follows

B.1.1 Theorem: 1

If C is a convex set and α is a real number, the set

$$\alpha C = \{x | x = \alpha c, c \in C\} \quad (\text{B.4})$$

B.1.2 Theorem: 2

If C and D are convex sets, the set

$$C + D = \{x | x = c + d, c \in C, d \in D\} \quad (\text{B.5})$$

B.2 The KUHN-TUCKER Conditions

Consider the following non-linear program problem that seeks an optimal x^*

$$\begin{aligned} & \max f(x) \\ & \text{subject to} \\ & g_j(x) \geq 0, \quad j = 1, \dots, r \\ & h_j(x) = 0, \quad j = 1, \dots, s \end{aligned} \quad (\text{B.6})$$

A maximization can always be transformed into minimization by multiplying the objective function by -1.

If x^* is the optimal point then there must exist a vector $\lambda \in R^r$

$$\lambda \geq 0 \tag{B.7}$$

and a vector $\mu \in R^s$ such that

$$\begin{aligned} \nabla f(x^*)^\tau + \sum_{j=1}^r \lambda_j \nabla g_j(x^*)^\tau + \sum_{j=1}^s \mu_j \nabla h_j(x^*)^\tau &= 0 \\ \lambda_j g_j(x^*) &= 0, \quad j = 1, \dots, r \end{aligned} \tag{B.8}$$

Observe that since x^* is optimal point, x^* also satisfies

$$\begin{aligned} g(x^*) &\geq 0 \\ h(x^*) &= 0 \end{aligned} \tag{B.9}$$

These equations are collectively known as K-T conditions.

REFERENCES

- [1] W. A. Mousa, “Seismic Migration: A Digital Filtering Process Reducing Oil Exploration Risks,” *IEEE signal processing magazine*, vol. 117, 2012.
- [2] D. Hale, “Stable explicit depth extrapolation of seismic wavefields,” *Geophysics*, vol. 56, pp. 1770–1777, 1991.
- [3] W. A. Mousa, M. van der Baan, S. Boussakta, and D. C. McLernon, “Designing stable operators for explicit depth extrapolation of 2-D and 3-D wavefields using projections onto convex sets,” *Geophysics*, vol. 74, pp. S33–S45, 2009.
- [4] R. J. Ferguson and G. F. Margrave, “Planned seismic imaging using explicit one-way operators,” *Geophysics*, vol. 70, pp. S101–S109, 2005.
- [5] W. A. Mousa, “Imaging of the SEG/EAGE Salt Model Seismic Data Using Sparse f-x Finite-Impulse-Response WaveField Extrapolation Filters,” *IEEE Transactions on Geoscience and remote sensing*, 2013.
- [6] J. F. Claerbout, “Imaging the earth’s interior,” *Blackwell Scientific Publications*, 1985.
- [7] R. Bracewell, *The Fourier Transform and its applications*, 1965.

- [8] A. J. Berkhout, *Imaging of acoustic energy by wavefield extrapolation*. Elsevier, 1982.
- [9] —, *Seismic resolution: resolving power of acoustic echo techniques*. Geophysical Press Ltd., 1984.
- [10] —, *Applied Seismic wave theory*. Elsevier, 1987.
- [11] —, *Pushing the limites of seismic imaging: part 1*. Geophysics, 1996a.
- [12] J. B. Diebold and P. L. Stoffa, “The travelttime equation, t–p mapping and inversion of common midpoint data,” *Geophysics*, vol. 46, pp. 238–254, 1981.
- [13] W. H. Dragoset and S. MacKay, “Surface multiple elimination and subsalt imaging,” *Expolation Geophysics*, vol. 24, pp. 463–472, 1993.
- [14] Gonzalez-Serrano, “Wave-equation velocity analysis,” Tech. Rep., 1982.
- [15] D. Hampson, “The discrete radon transform: A new tool for image enhancement and noise suppression,” *Expolation Geophysics*, vol. 57, pp. 141–143, 1987.
- [16] P. Hubral and T. Krey, “Interval velocities from seismic reflection time measurements,” *Society of Expolation Geophysics*, 1980.
- [17] I. F. Jones and S. Levy, “Signal-to-noise ratio enhancement in multichannel seismic data via the karhunen-loeve transform,” *Geophysics*, vol. 35, pp. 12–32, 1987.

- [18] P. G. Kelamis and A. R. Mitchell, *Slant-stack processing: First Break*, 1989.
- [19] J. Gazdag, “Wave equation migration with the phase-shift method,” *Geophysics*, vol. 43, pp. 1342–1351, 1978.
- [20] J. Gazdag and P. Sguazzero, “Migration of seismic data by phase shift plus interpolation,” *Geophysics*, vol. 49, pp. 124–131, 1984.
- [21] L. R. Lines and S. Treitel, “A review of least-squares inversion and its application to geophysical problems,” *Geophysics*, vol. 32, pp. 159–186, 1984.
- [22] Ottolini, R, “Migration of seismic data in angle-midpoint coordinates,” Tech. Rep., 1982.
- [23] W. S. French, “Two-dimensional and three-dimensional migration of model experiment reflection profiles,” *Geophysics*, vol. 39, pp. 265–277, 1974.
- [24] —, “Computer migration of oblique seismic reflection profiles,” *Geophysics*, vol. 40, pp. 961–980, 1975.
- [25] C. Esmersoy and M. L. Oristaglio, “Reverse-time wave-field extrapolation, imaging and inversion,” *Geophysics*, vol. 1, pp. 97–106, 1988.
- [26] D. C. Riley and J. F. Claerbout, “2-d multiple reflections,” *Geophysics*, vol. 41, pp. 592–620, 1976.
- [27] O. Holberg, “Towards optimum one-way wave propagation,” *Geophys*, vol. 36, pp. 99–114, 1988.

- [28] L. J. Karam and J. H. McClellan, "Efficient design of digital filters for 2-D and 3-D depth migration," *IEEE Trans. Signal Processing*, vol. 45, pp. 1036–1044, 1997.
- [29] J. W. Thorbecke, K. Wapenaar, and G. Swinnen, "Design of one-way wavefield extrapolation operators, using smooth functions in WLSQ optimization," *Geophysics*, vol. 69, pp. 1037–1045, 2004.
- [30] G. F. Margrave and R. J. Ferguson, "Taylor series derivation of nonstationary wavefield extrapolators," CREWES Research Report, Tech. Rep., 1999.
- [31] W. A. Mousa, "The design of stable, sparse wavefield extrapolators using projections onto convex sets," *Geophysics*, vol. 78, pp. T11–T20, 2012.
- [32] . Yilmaz, Ed, *Seismic Data Analysis: Processing, Inversion, and Interpretation of Seismic Data*. Society of Exploration Geophysicists, 2001.
- [33] Gary Stuart Martin, "The marousi2 model, elastic synthetic data, and an analysis of imaging and avo in a structurally complex environment," Tech. Rep., 2004.
- [34] Thorbecke, "Common focus point technology," Delft University of Technology, Tech. Rep., 1997.
- [35] D. Hale, "3D migration via McClellan transformation," *Geophysics*, vol. 56, pp. 1778–1785, 1991.

- [36] Hedley, “3-D migration via McClellan transformations hexagonal grids,” *Geophysics*, vol. 57, pp. 1048–1053, 1992.
- [37] J. G. Proakia and D. G. Manolakis, *Digital signal processing principals, algorithms and applications*. Pearson Prentice Hall.
- [38] G. Murty, *Linear Complementarity: Linear and Nonlinear Programming*, 1997.
- [39] R. W. Cottle, J.-S. Pang, and R. E. Stone, *The Linear Complementarity Problem*, 2009.
- [40] O. L. Mangasarain, “Equivalence of the complementarity problem to a system of nonlinear equations,” *Journal on Applied Mathematics*, vol. 31, pp. 89–92, 1976.
- [41] D. den Hertog, C. Roos, and T. Terlaky, “The linear complementarity problem, sufficient matrices and the crisscross method,” *Linear Algebra*, vol. 187, pp. 1–14, 1993.
- [42] K. Fukuda, M. Namiki, and A. Tamura, “Ep theorems and linear complementarity problems,” *Discrete Appl. Math*, vol. 84, pp. 107–119, 1998.
- [43] A. Fischer, “A newton-type method for positive-semi definite linear complementarity problems,” *Journal of Optimization Theory and Applications*, vol. 86, pp. 585–608, 1995.

- [44] O. L. Mangasarain, “Locally unique solutions of quadratic programs, linear, and nonlinear complementarity problems,” *Journal on Applied Mathematics*, vol. 19, pp. 200–212, 1980.
- [45] M. Aganagic, “Newton’s method for linear complementarity problems,” *Mathematical Programming*, vol. 28, pp. 349–362, 1984.
- [46] L. T. Watson, “Solving the nonlinear complementarity problem by a homotopy method,” *SIAM Journal on Control and Optimization*, vol. 17, pp. 36–46, 1979.
- [47] P. T. Harker and J. S. Pang, “A damped newton method for the linear complementarity problem,” *Lectures in Applied Mathematics*, vol. 26, pp. 265–284, 1990.
- [48] M. Kojima, S. Mizuno, and T. Noma, “A new continuation method for complementarity problems with uniform p-functions,” *Mathematical Programming*, vol. 43, pp. 107–114, 1989.
- [49] P. T. Harker and B. Xiao, “Newton’s method for the nonlinear complementarity problem: A b-differentiable equation approach,” *Mathematical Programming*, vol. 48, pp. 339–357, 1990.
- [50] B. Jansen, C. Roos, and T. Terlaky, “A family of polynomial affine scaling algorithms for positive semidefinite linear complementarity problems,” *SIAM J. Optim*, vol. 7, pp. 126–140, 1996.

- [51] A. M. A.-F. Nuseirat, “Design of linear phase fir filters via linear complementarity problem approach,” *International Journal Of Circuit Theory And Application*, vol. 33, pp. 353–364, 2005.
- [52] A. A.-F. Nuseirat and R. Abu-Zitar, “Fir filter design via linear complementarity problem, messy genetic algorithm, and using messy genetic algorithm,” *World Academy of Science, Engineering and Technology*, 2007.
- [53] W. I. Zangwill and C. B. Garcia, *Pathways to solutions, fixed points and Equilibria*, 1981.

Vitae

- Name: Muhammad Muzammal Naseer
- Nationality: Pakistani
- Date of Birth: 09/01/1986
- Email: *muz.pak@gmail.com*
- Permenant Address: Habib Town, House No:118, Plot No:12-13, Sahiwal,
Pakistan